multiphoton multielectron ionization to high charge states & high-definition X-ray polarimetry

G. G. Paulus
Institute of Optics and Quantum Electronics, Friedrich Schiller University Jena, Germany
Helmholtz Institute Jena, Germany

A. M. Sayler, P. Wustelt, M. Möller, S. Trotsenko, W. Quint, T. Stöhlker
B. Marx, K.-S. Schulze, H. Bernhardt, B. Grabiger, I. Uschmann

- ionization of ions
  - ion beam apparatus
  - experiments with Ne^{+}
  - future directions
- high-definition X-ray polarimetry
  - Si channel-cuts
  - diamond quasi channel-cuts

new target: ions

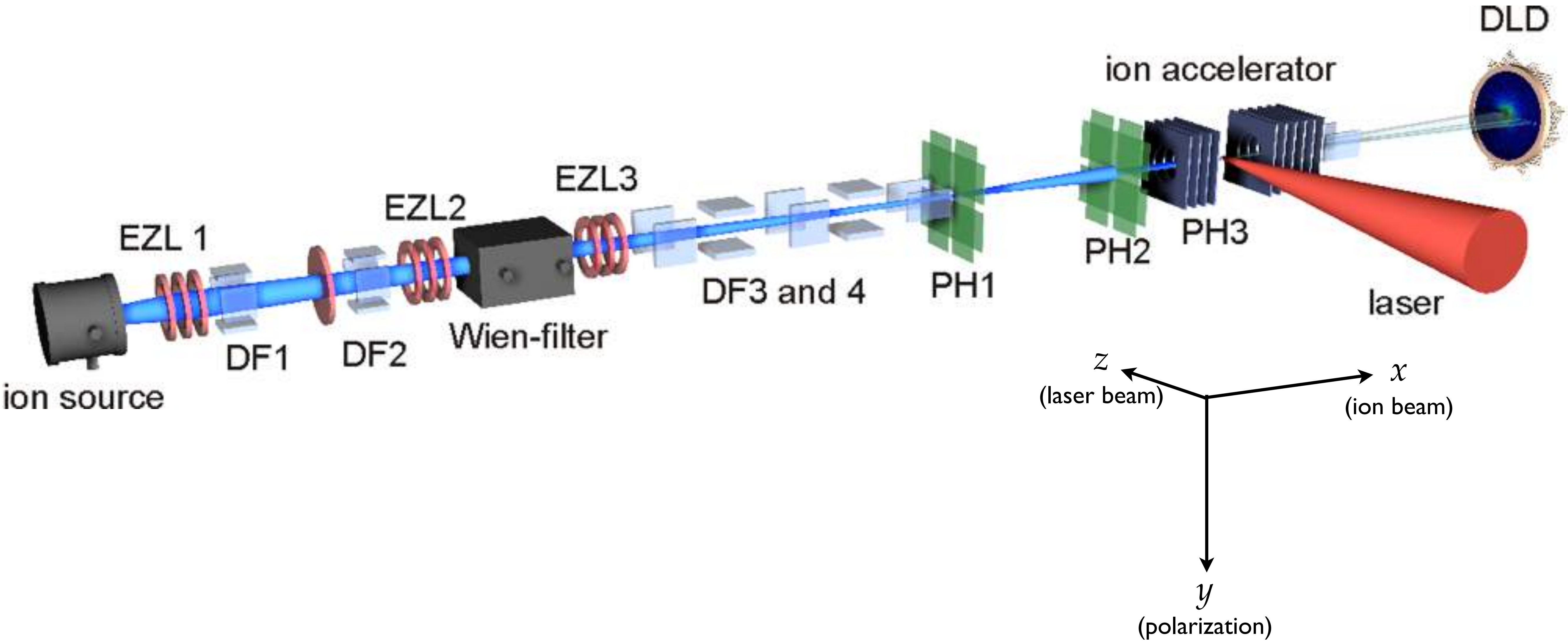

ionization of Xe^{+}

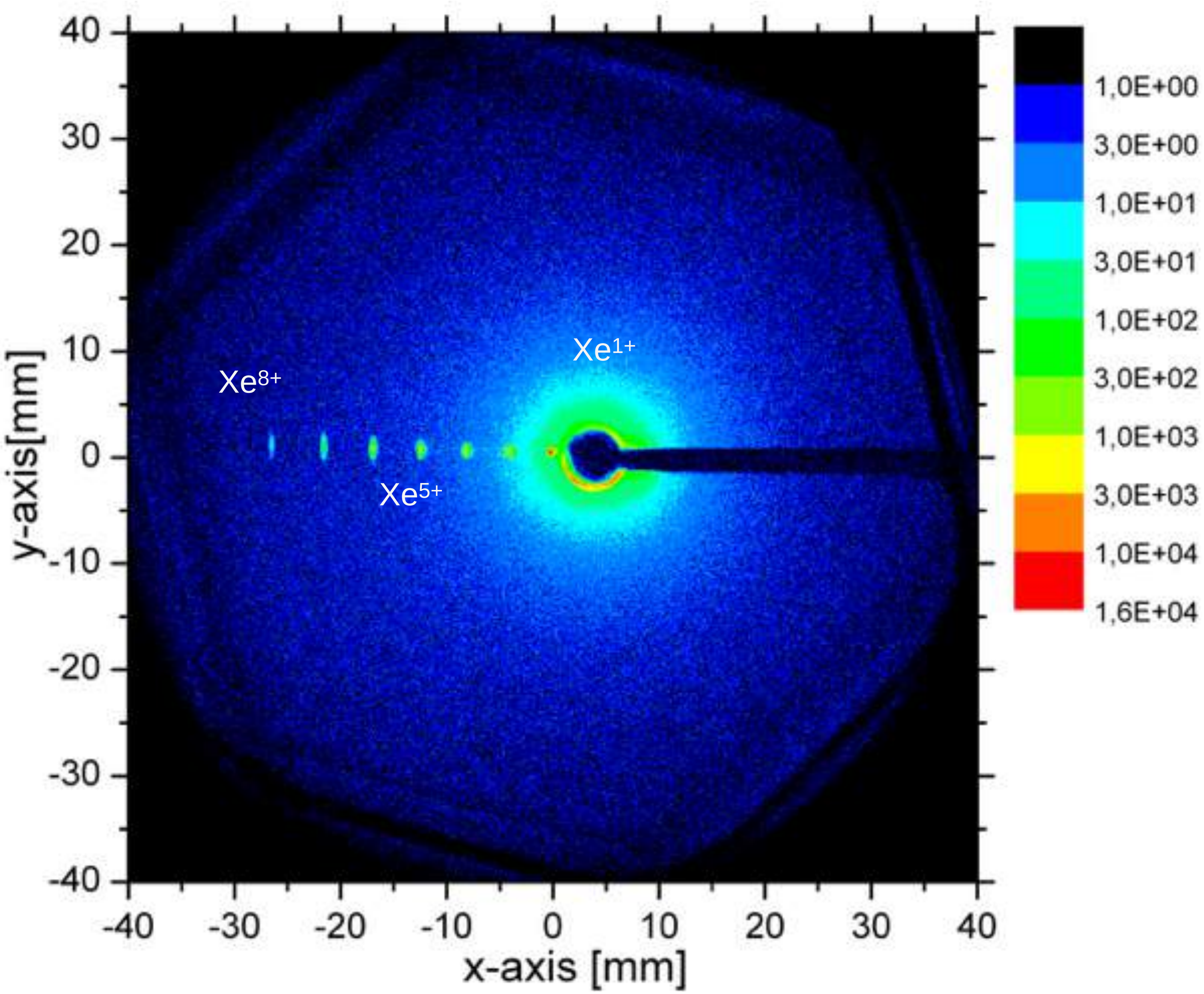

ionization of Ne^{+}

Ne^{2+}

Ne^{3+}

Ne^{4+}

Ne^{5+}

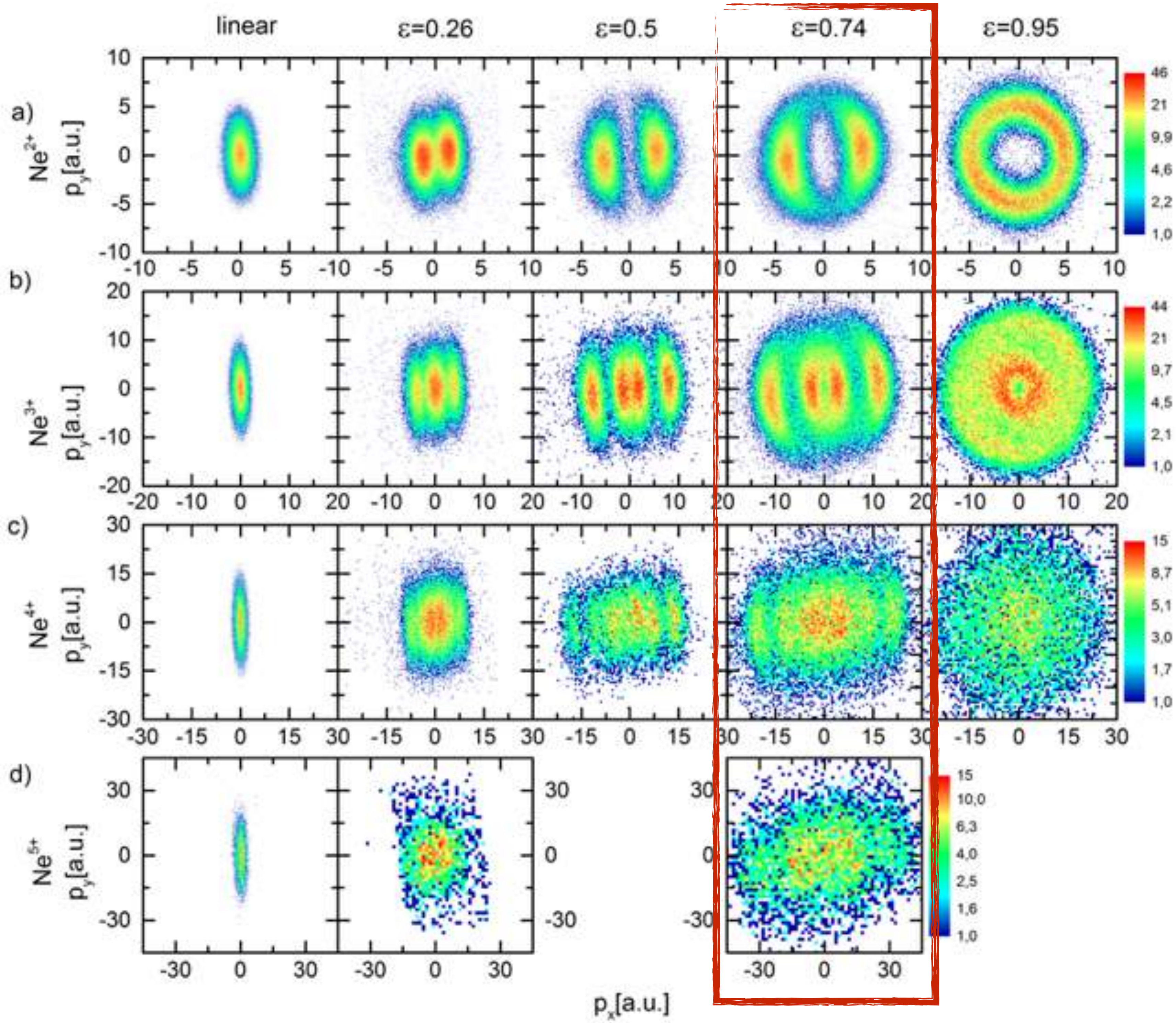

Ph. Wustelt et al., *Phys. Rev. A* **91**, 031401 (2015)

ionization of Ne^{+}

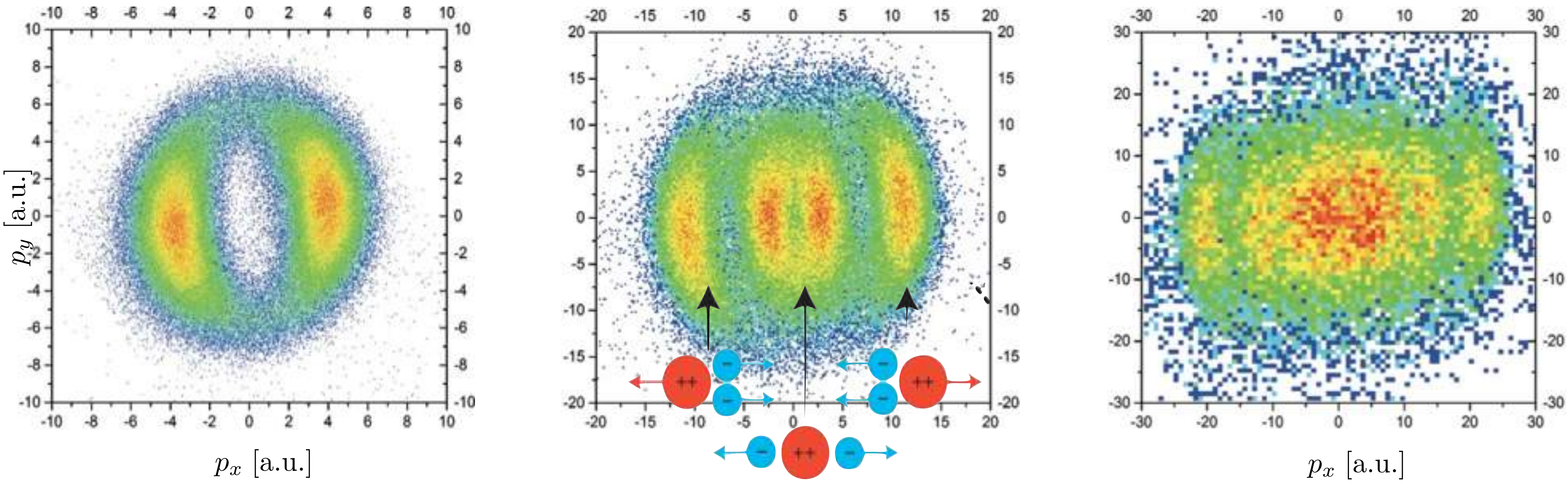

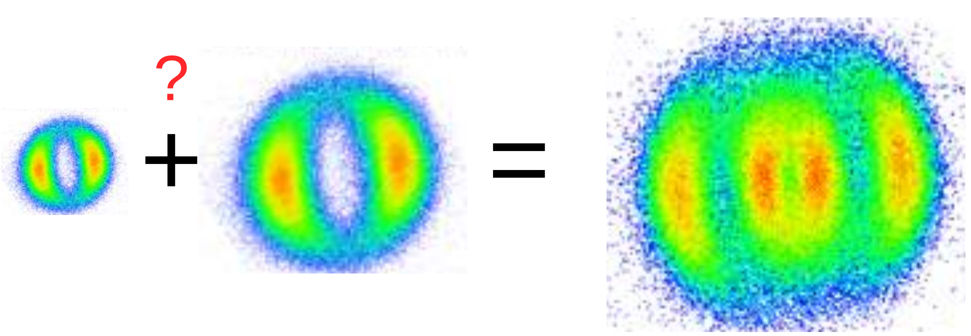

Ph. Wustelt et al., *Phys. Rev. A* **91**, 031401 (2015)

parametrization of single ionization

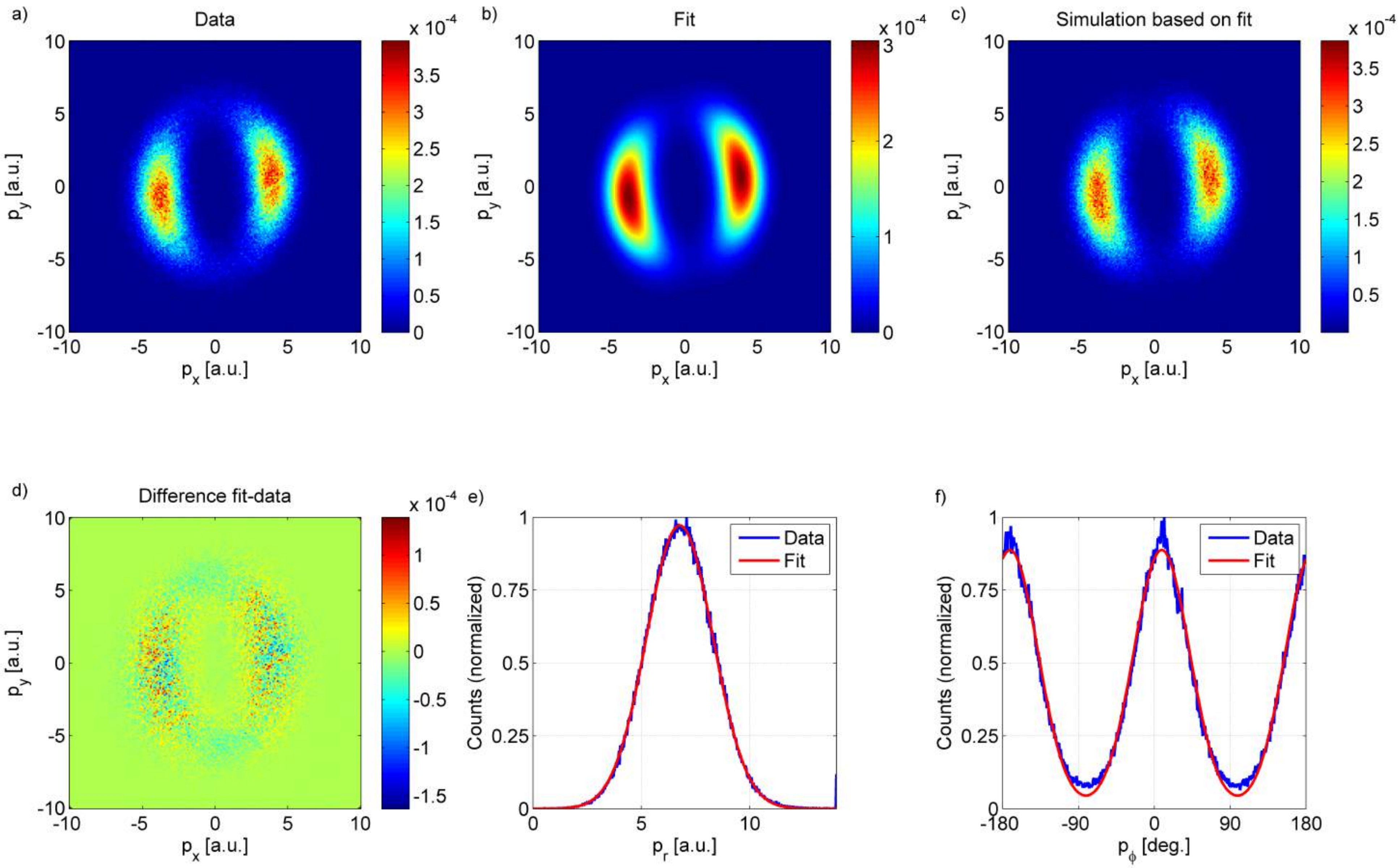

$$F_{\text{single}}(p_r, p_\phi) := \frac{1}{p_r}\,\exp\left[-\left(\frac{p_r - p_{r_0}}{\Delta p_r}\right)^2\right]\,\exp\left[-\left(\frac{p_\phi - p_{\phi_0}}{\Delta p_\phi}\right)^2\right]$$

Ph. Wustelt et al., *Phys. Rev. A* **91**, 031401 (2015)

parametrization of double ionization

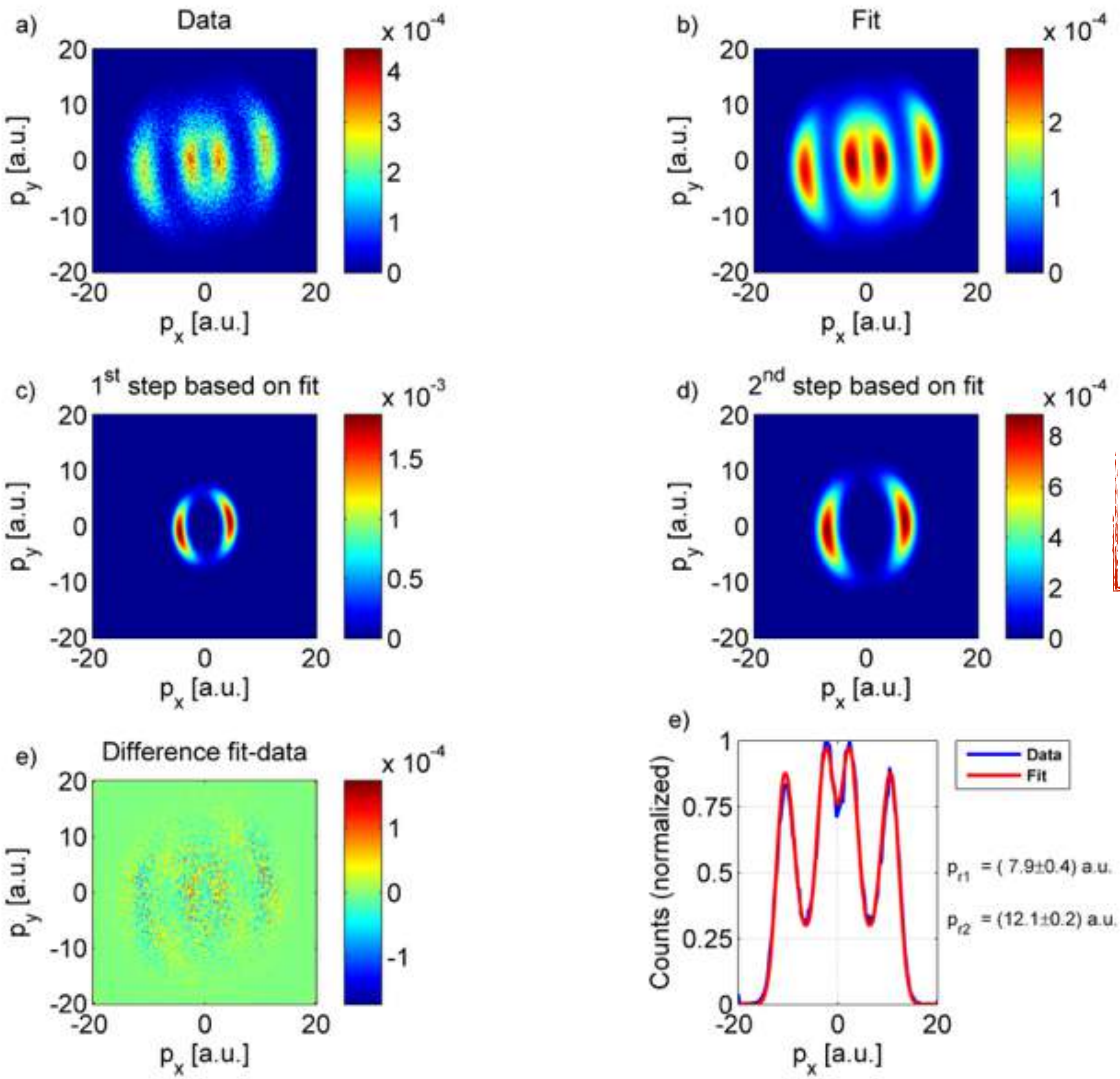

$$F_{1\to3}(p_r, p_\phi) \;=\; F_{1\to2} * F_{2\to3}$$

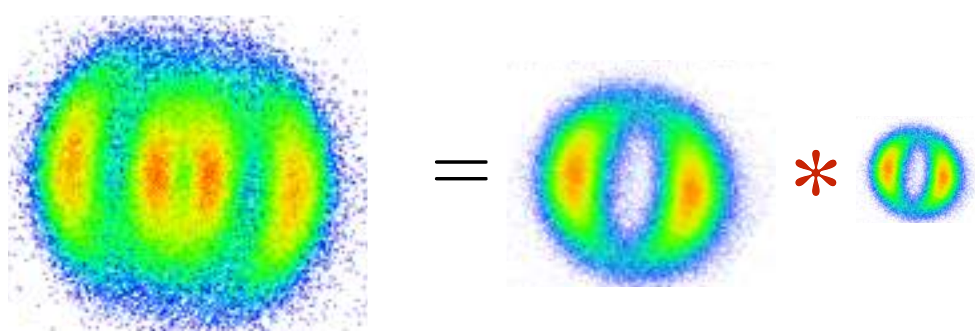

Ph. Wustelt et al., *Phys. Rev. A* **91**, 031401 (2015)

dynamics of multiple ionization

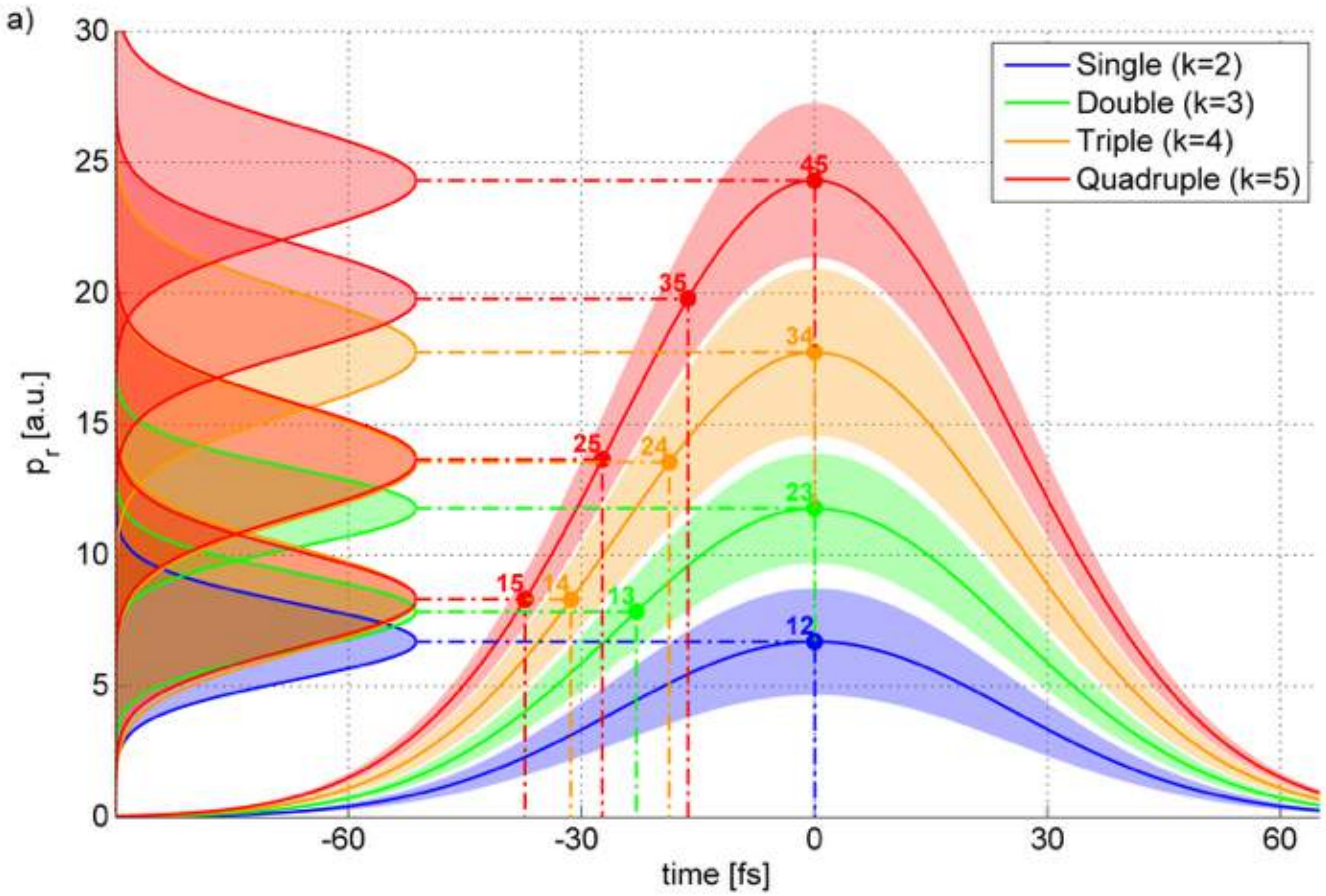

Ph. Wustelt et al., *Phys. Rev. A* **91**, 031401 (2015)

saturation intensity & theory

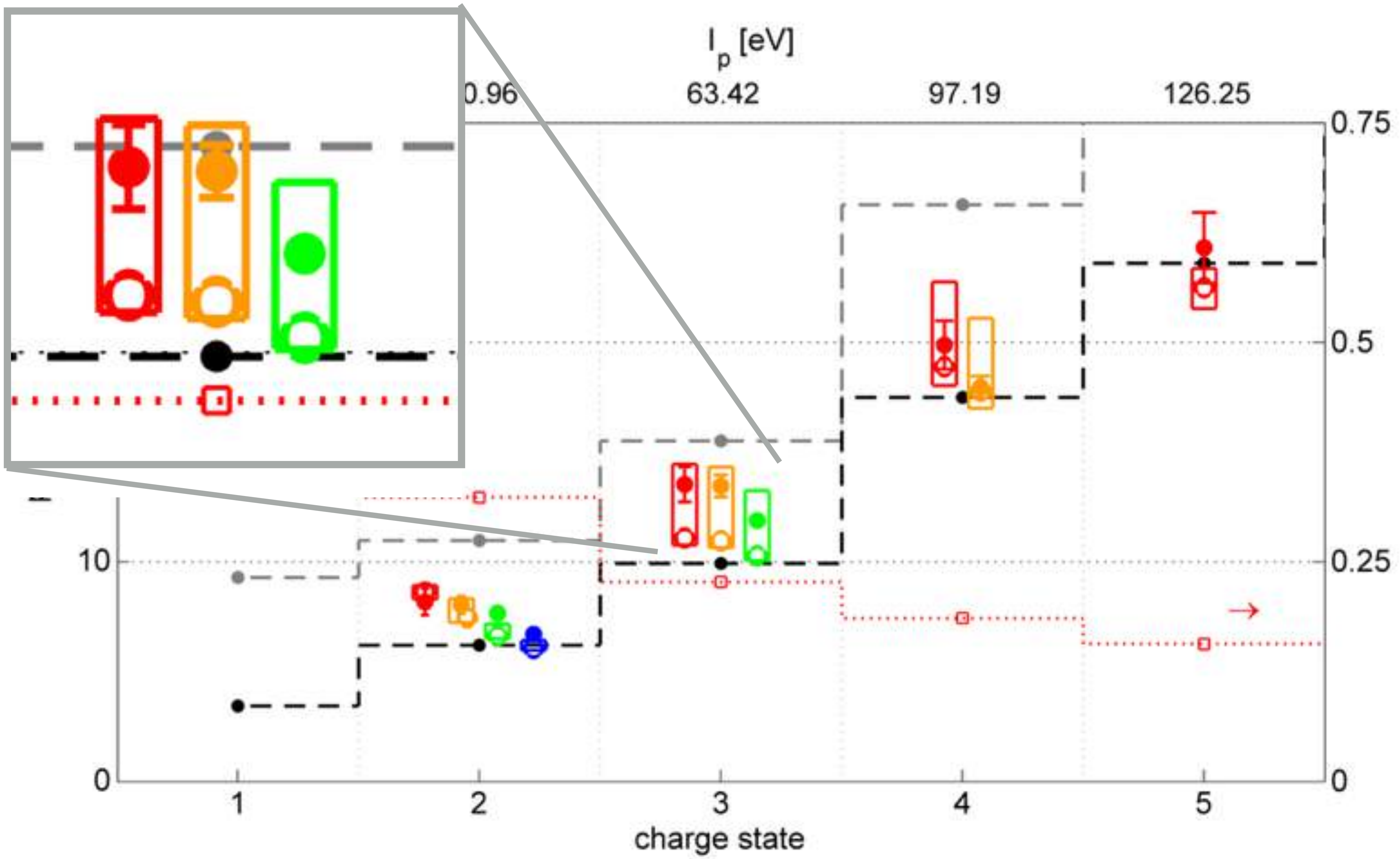

$$\dot{P} = \frac{C}{2^m\, m!} \times \frac{1}{\kappa^{2Z/\kappa-1}} \times \left(\frac{2\,\kappa^3}{\mathcal{E}}\right)^{2Z/\kappa-1} \times \exp\left[-\frac{2\,\kappa^3}{3\,\mathcal{E}}\right]$$

Ph. Wustelt et al., *Phys. Rev. A* **91**, 031401 (2015)

ionization of He^{+}: *ab initio* intensity measurement

$$\gamma = 0.125 \ldots 0.25$$

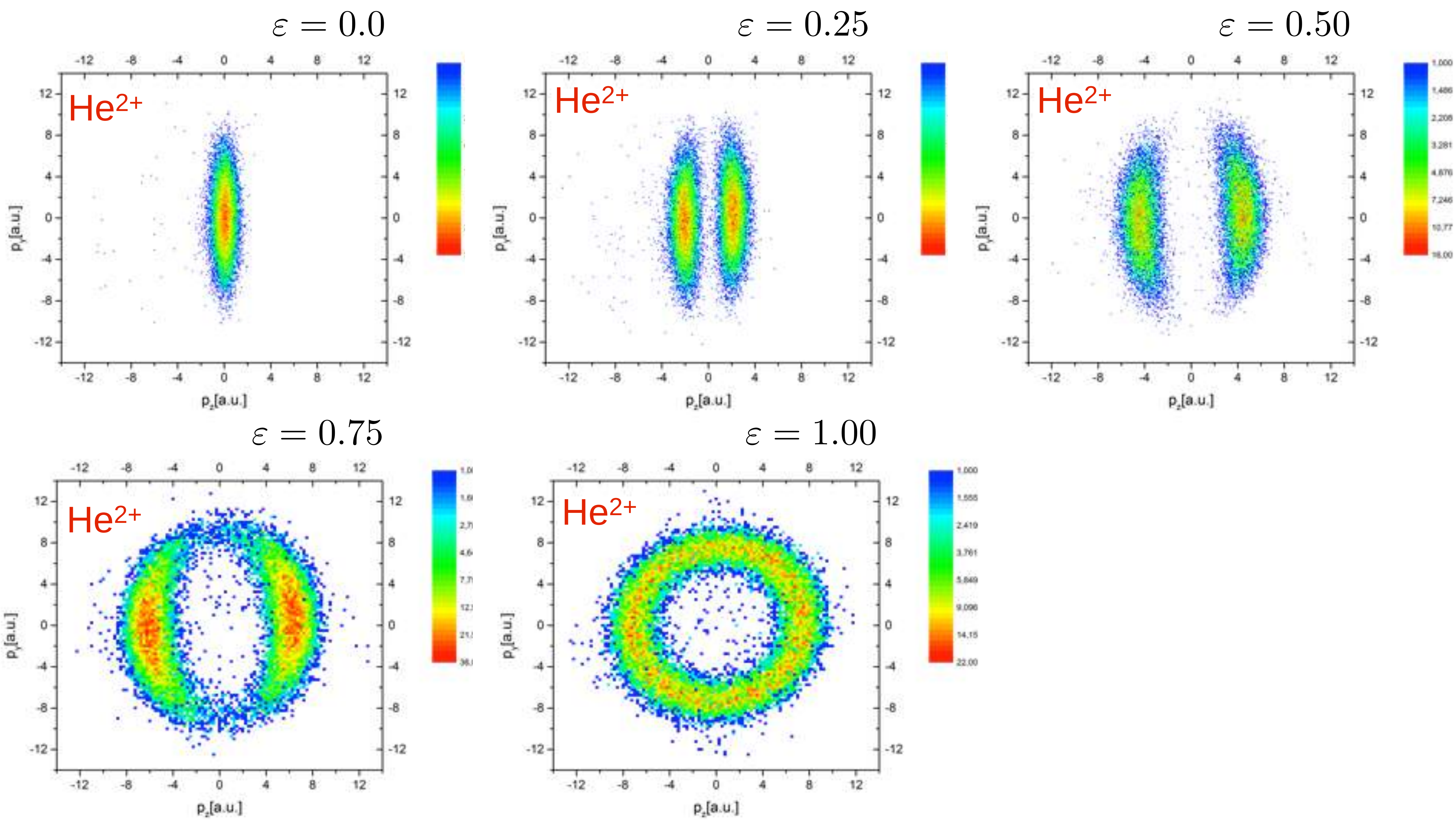

ionization of He^+: *ab initio* intensity measurement

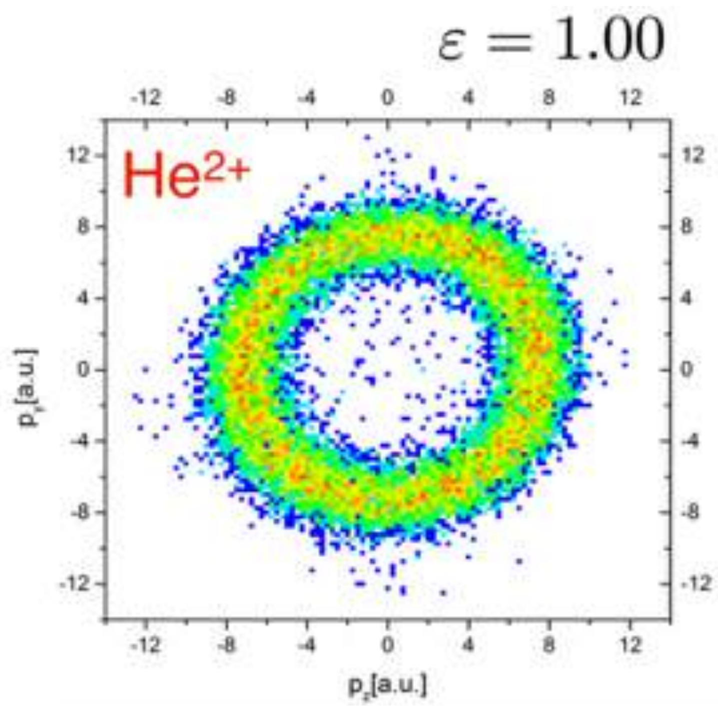

He$^+$: $I_{\text{sat}} \approx 10^{16}\,\text{W/cm}^2$

Ne^{9+}: $I_{\text{sat}} \approx 10^{20}\,\text{W/cm}^2$

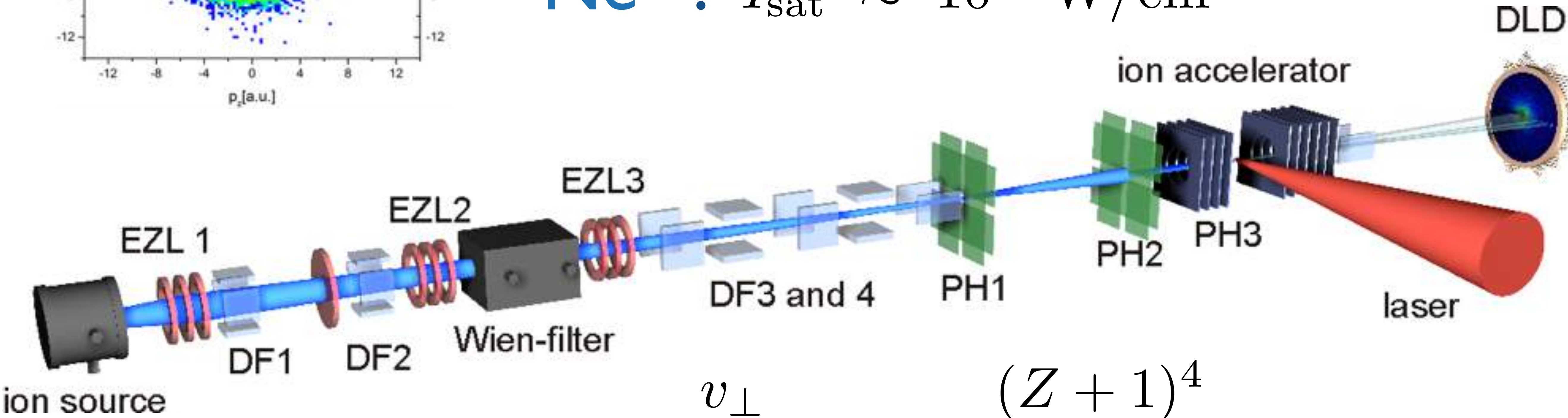

$$\frac{v_\perp}{v_\parallel} \approx \frac{(Z+1)^4}{1\,500\,\sqrt{Z(Z+1)}}$$

ionization of He^{+}: *ab initio* intensity measurement

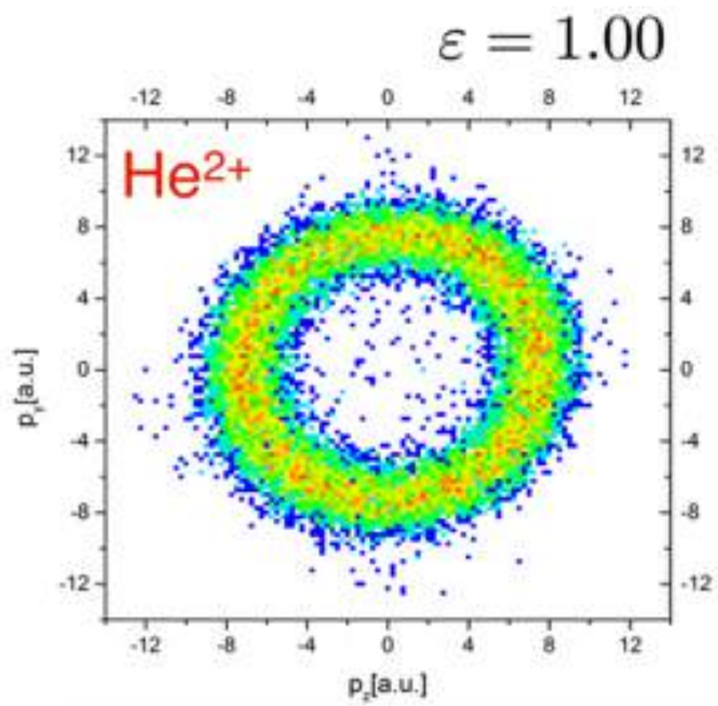

$$\mathrm{He}^{+}: \quad \frac{v_\perp}{v_\parallel} \approx \frac{1}{200}$$

$$\mathrm{Ne}^{9+}: \quad \frac{v_\perp}{v_\parallel} \approx \frac{1}{2}$$

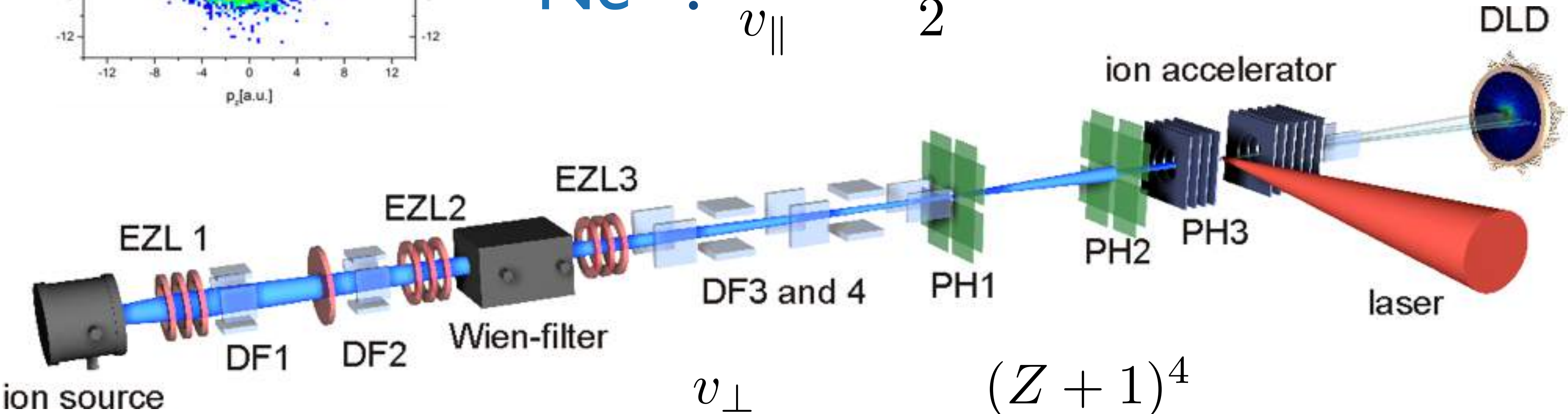

$$\frac{v_\perp}{v_\parallel} \approx \frac{(Z+1)^4}{1\,500\,\sqrt{Z(Z+1)}}$$

- ionization of ions
  - ion beam apparatus
  - experiments with Ne^{+}
  - future directions
- high-definition X-ray polarimetry
  - Si channel-cuts
  - diamond quasi channel-cuts

high-definition X-ray polarimetry: why?

- analytics
- nuclear resonant scattering
- Faraday rotation in overdense plasma
- vacuum birefringence

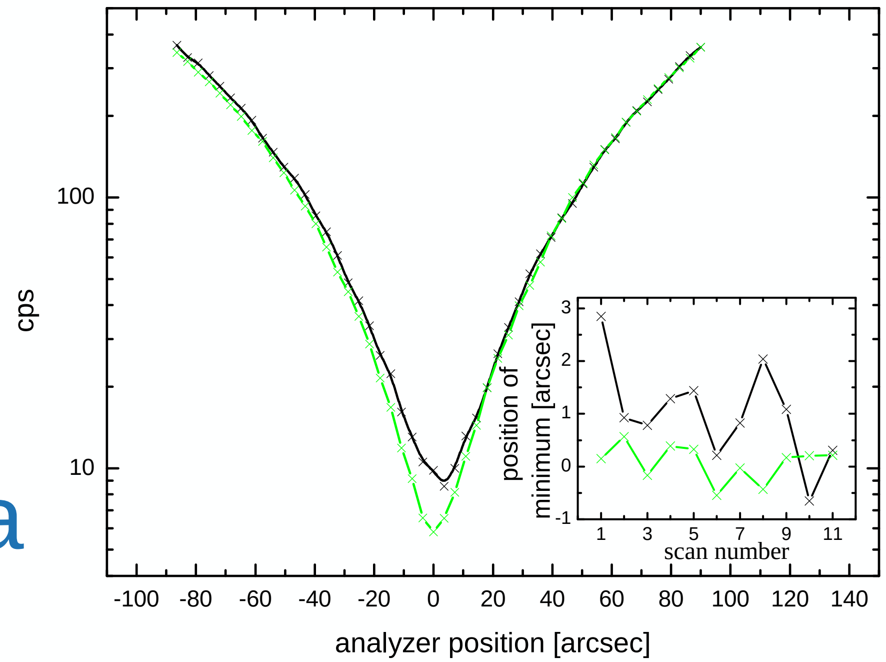

X-ray optical activity of sugar
[Marx et al., Phys. Rev. Lett. **110**, 254801 (2013)]

high-definition X-ray polarimetry: why?

- analytics
- nuclear resonant scattering
- Faraday rotation in overdense plasma
- vacuum birefringence

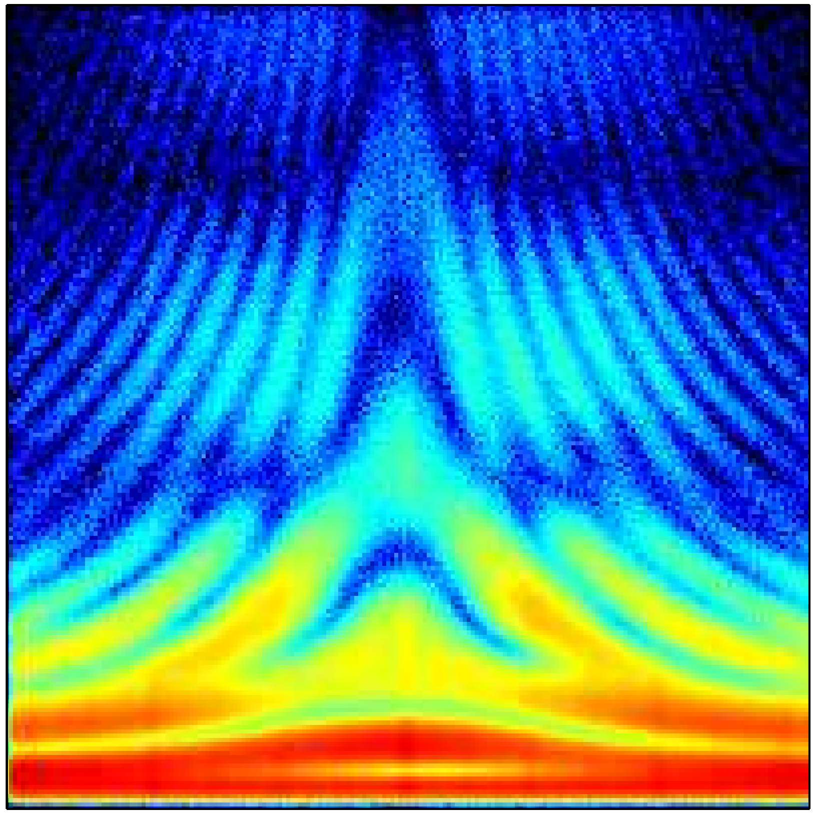

slow X-ray photons
[Heeg et al., Phys. Rev. Lett. **114**, 203601 (2015)]

high-definition X-ray polarimetry: why?

- analytics
- nuclear resonant scattering
- Faraday rotation in overdense plasma
- vacuum birefringence

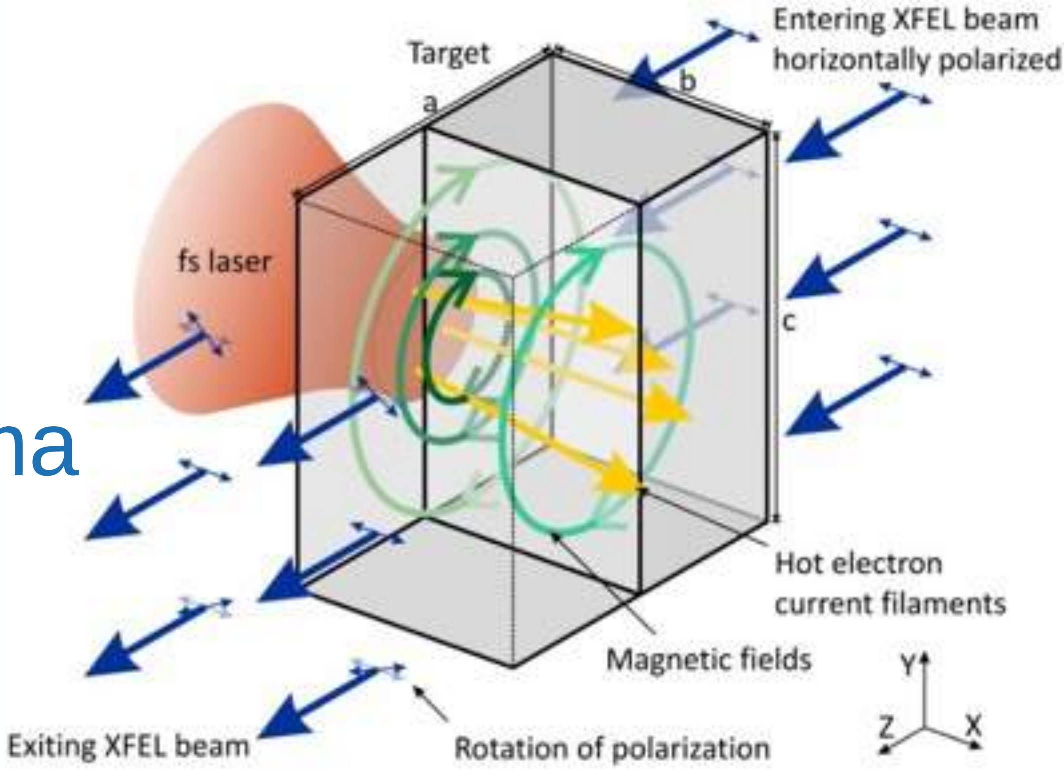

Faraday Rotation [Schlenvoigt Proposal LCLS 2014]

high-definition X-ray polarimetry: why?

- analytics
- nuclear resonant scattering
- Faraday rotation in overdense plasma
- vacuum birefringence

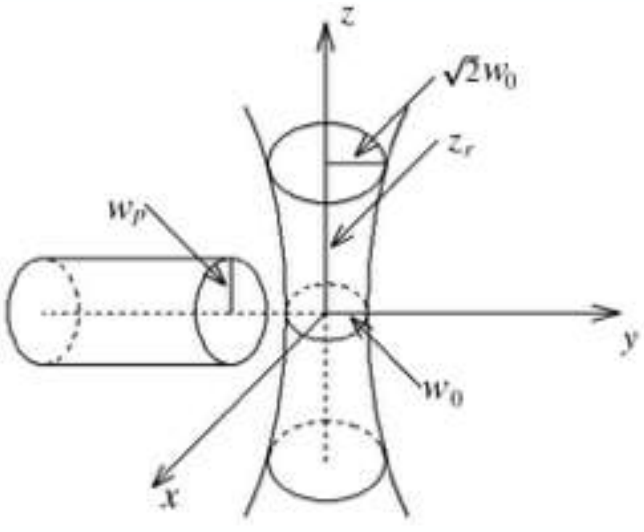

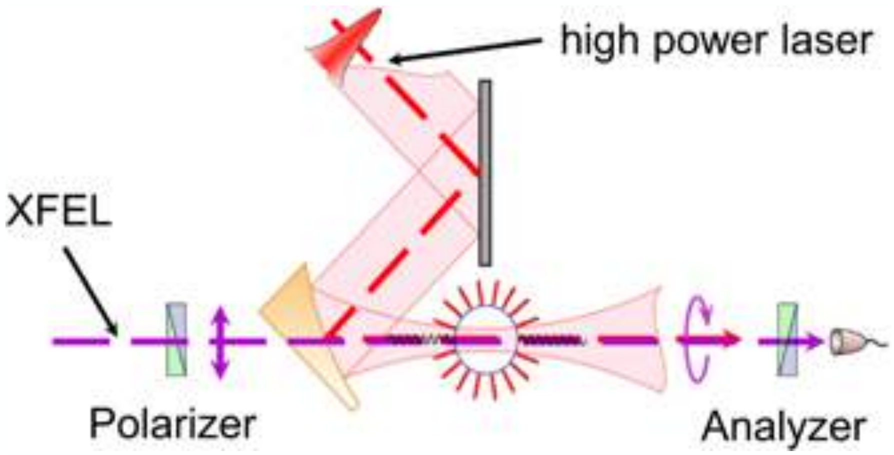

[Di Piazza *et al.* Phys. Rev. Lett. **97**, 083603 (2006)]

[T. Heinzl *et al*. Optics Communications **267**, 318 (2006)]

high-purity X-ray polarizer

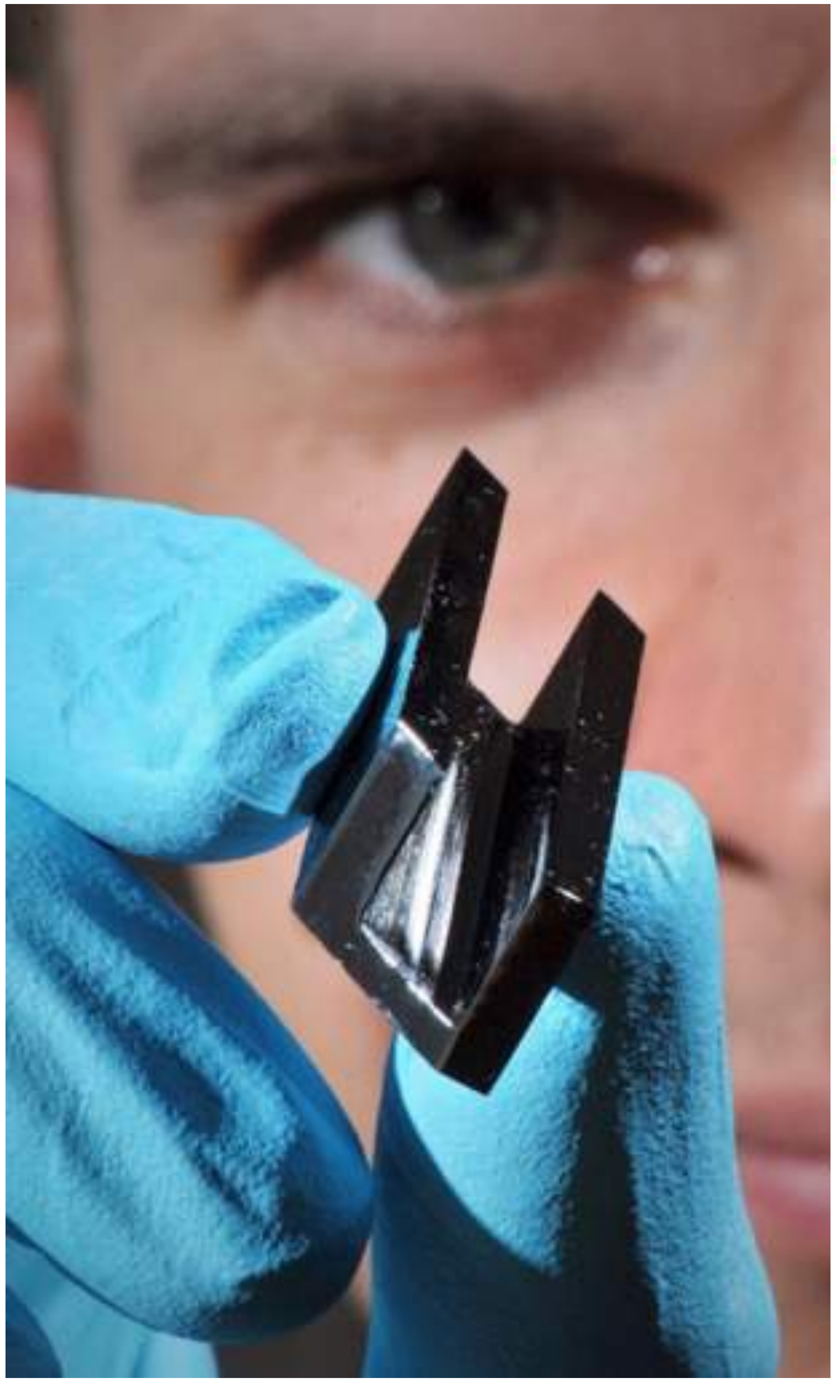

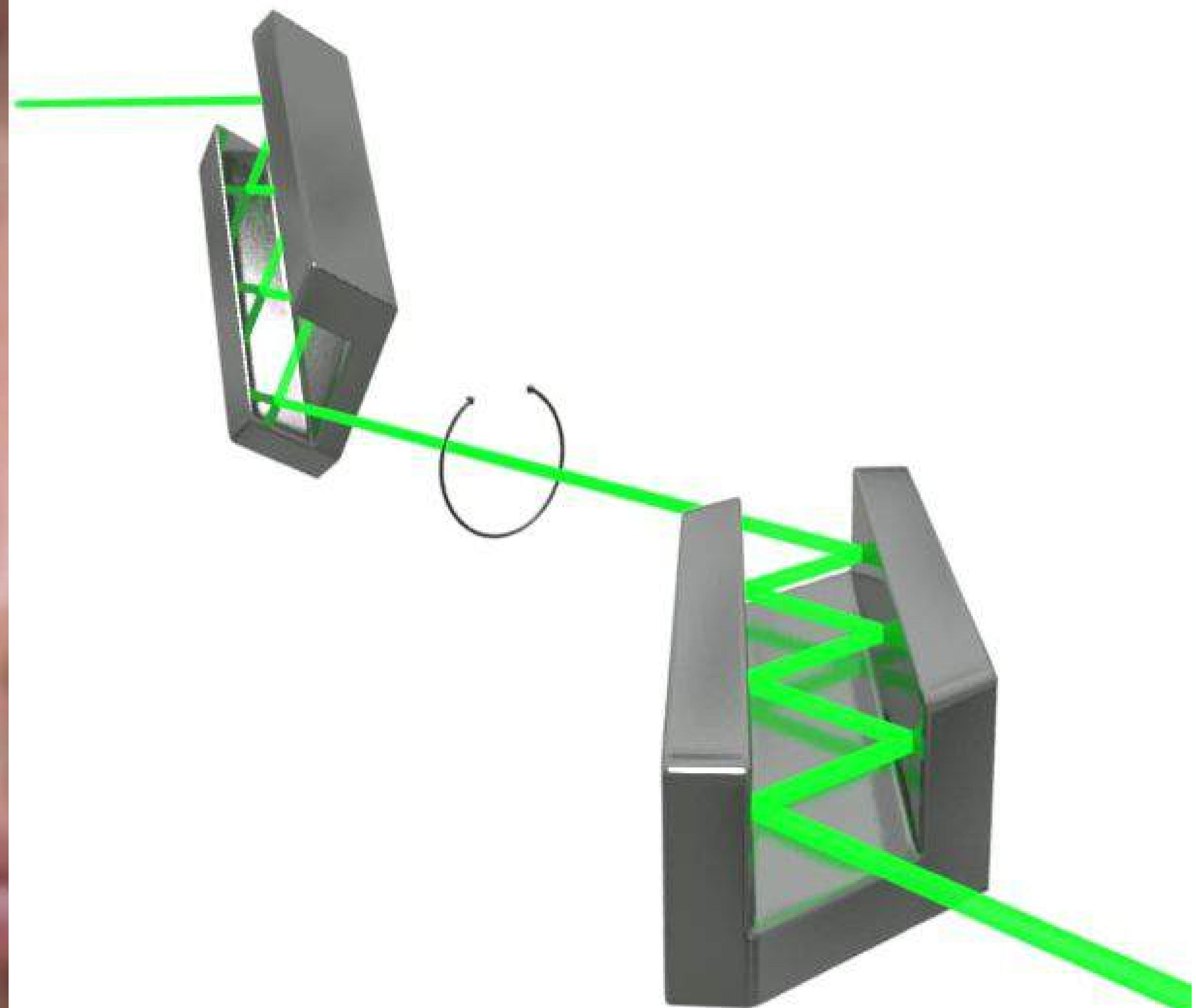

high-purity X-ray polarizer: Brewster effect

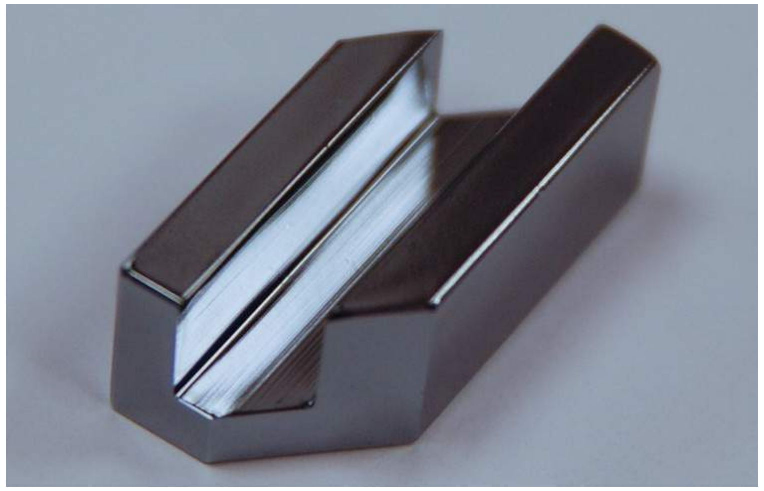

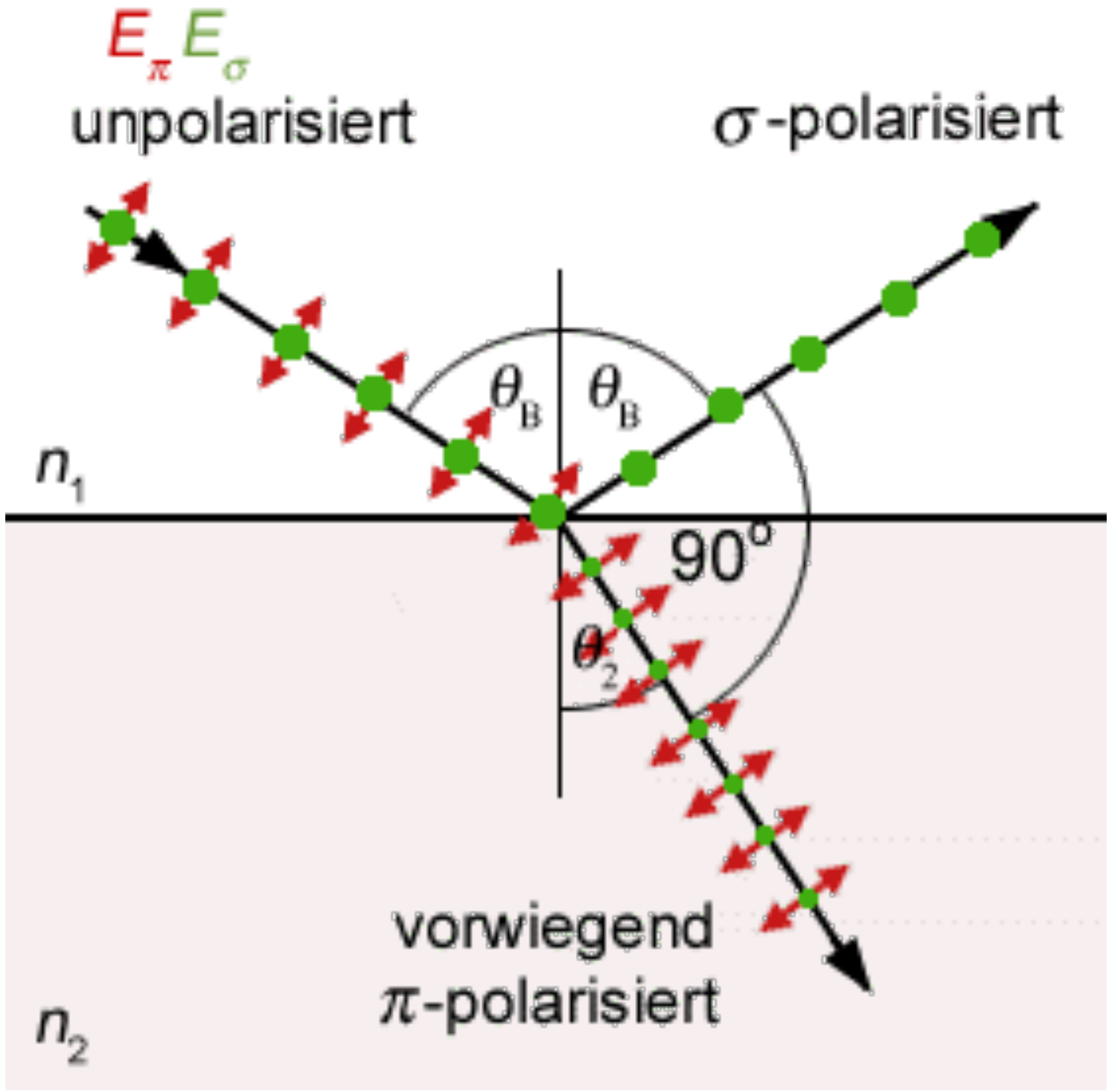

high-purity X-ray polarizer

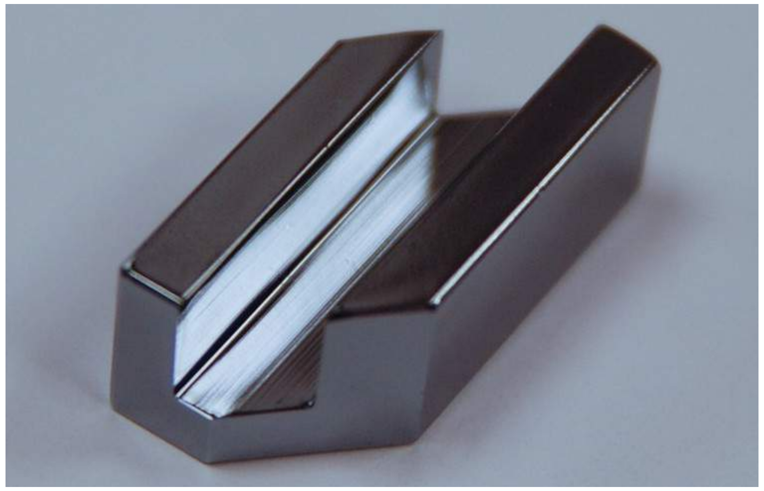

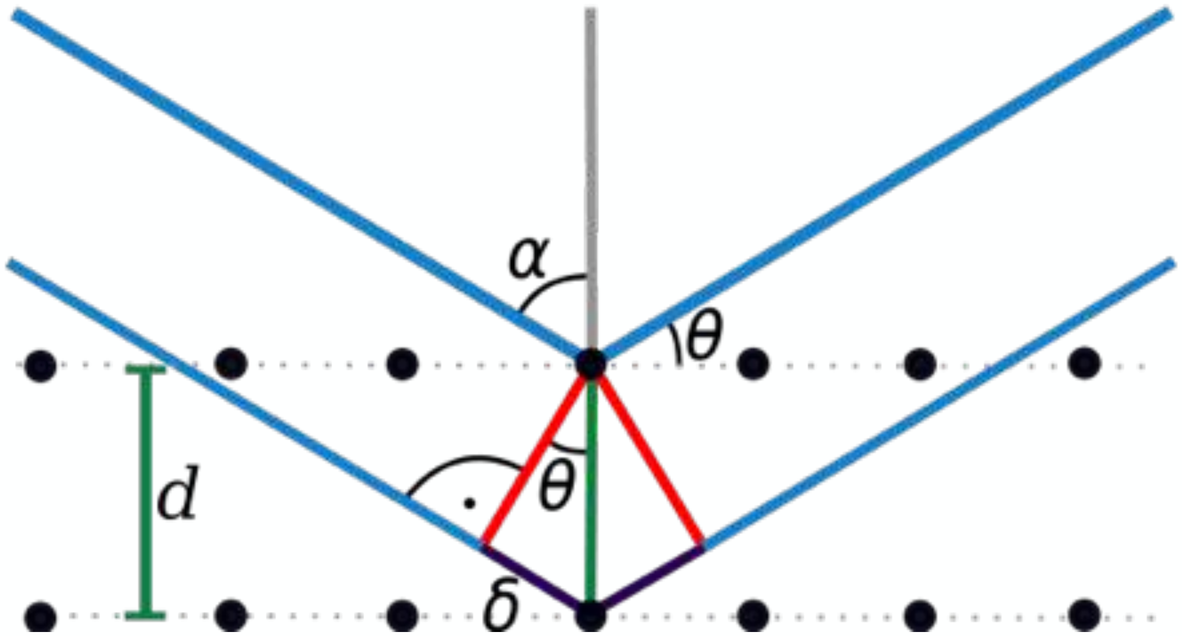

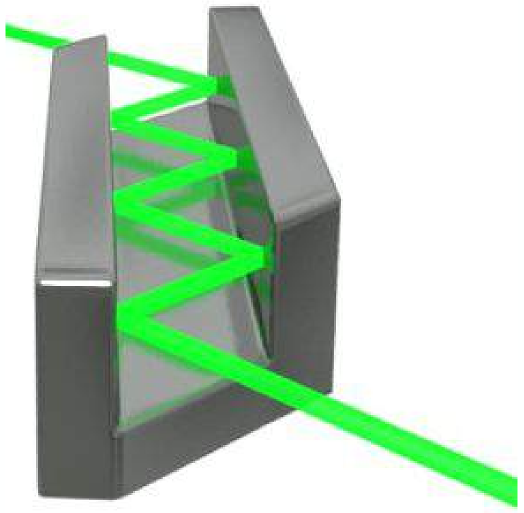

high-purity X-ray polarizer

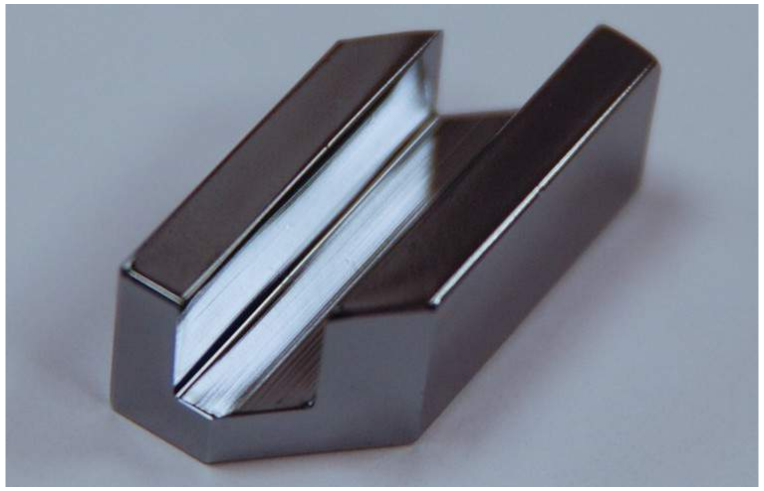

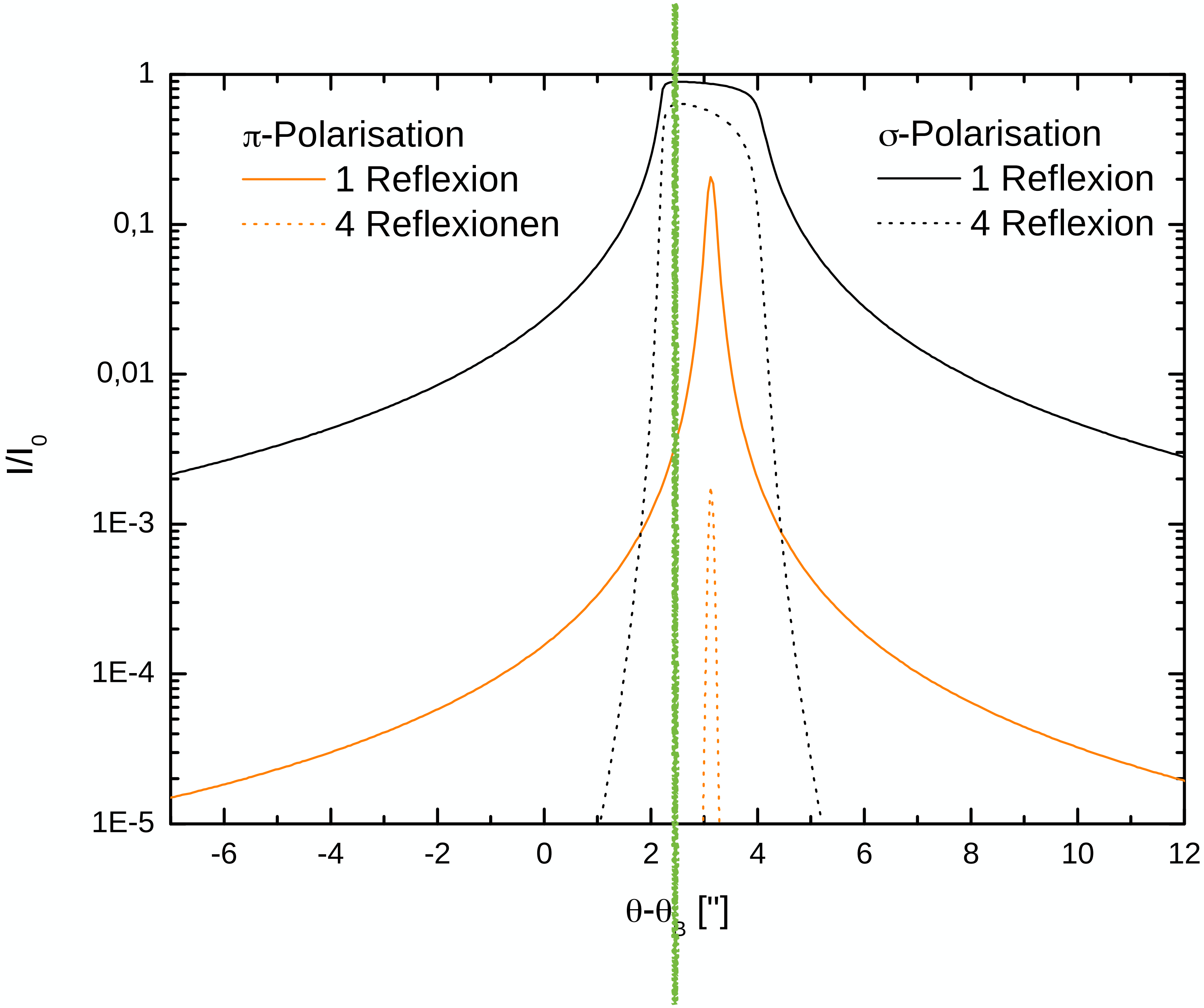

experimental setup

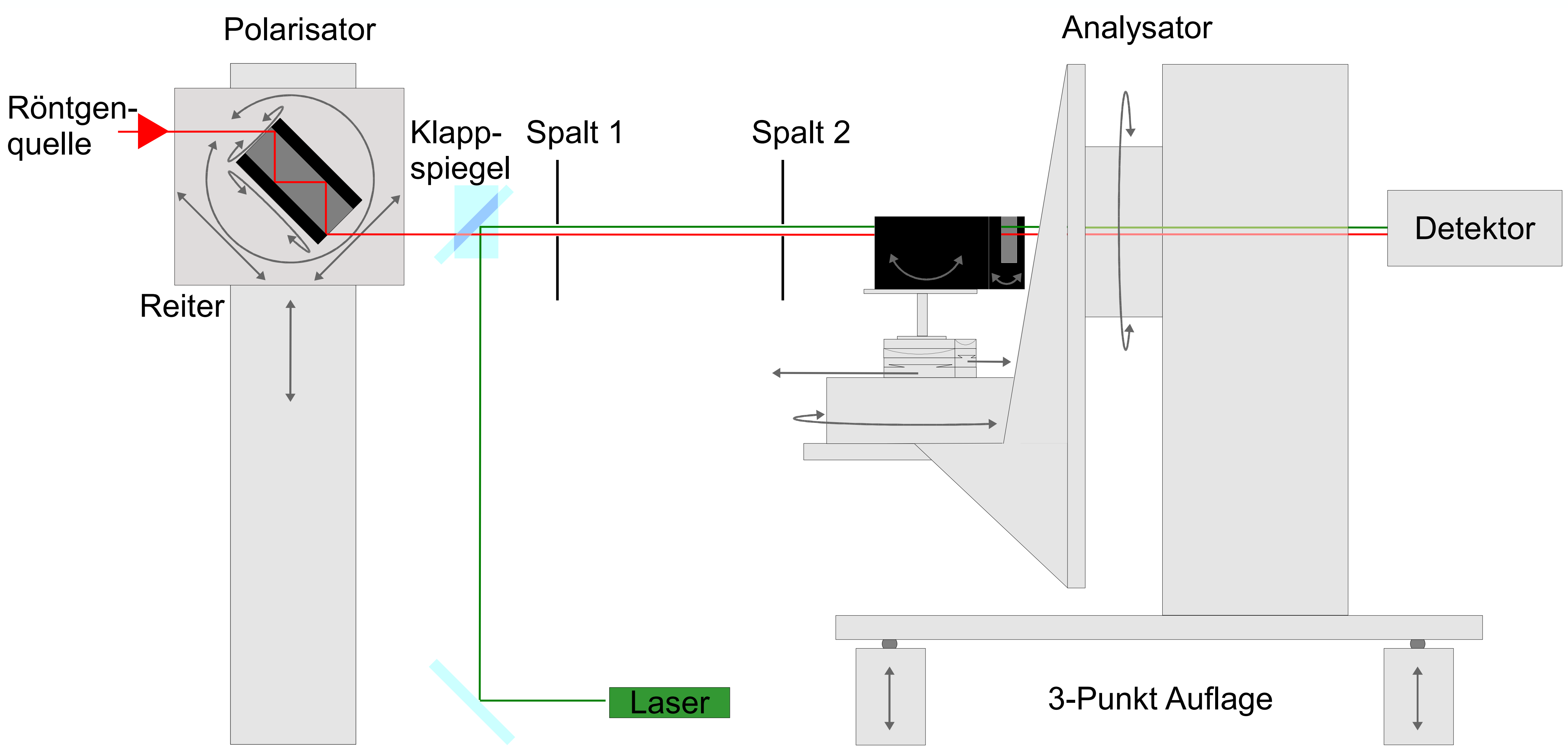

extinction curve

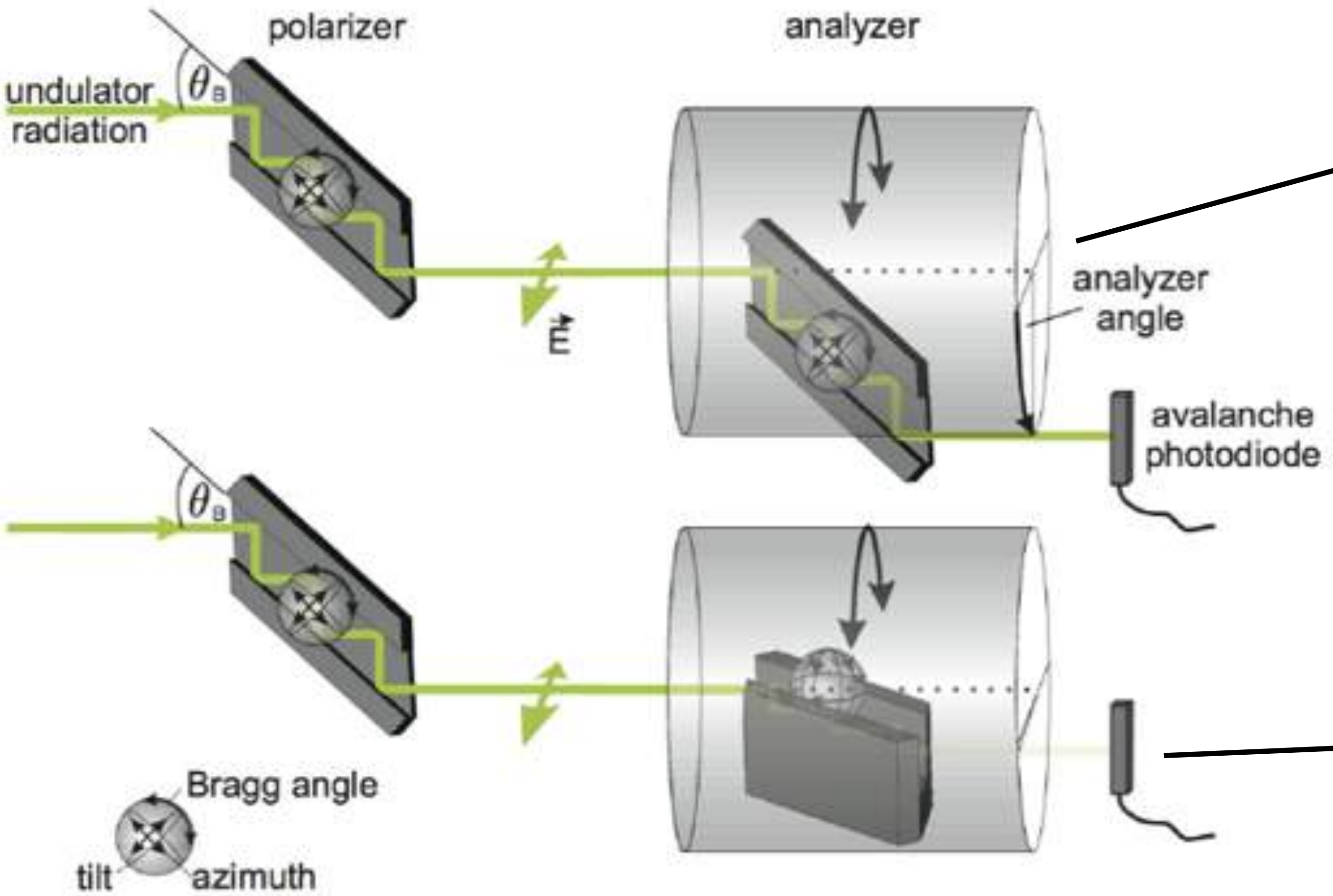

Fig. 8: Scheme of the polarizer and analyzer setup with analyzer in transmission (top) and analyzer in suppression (bottom)

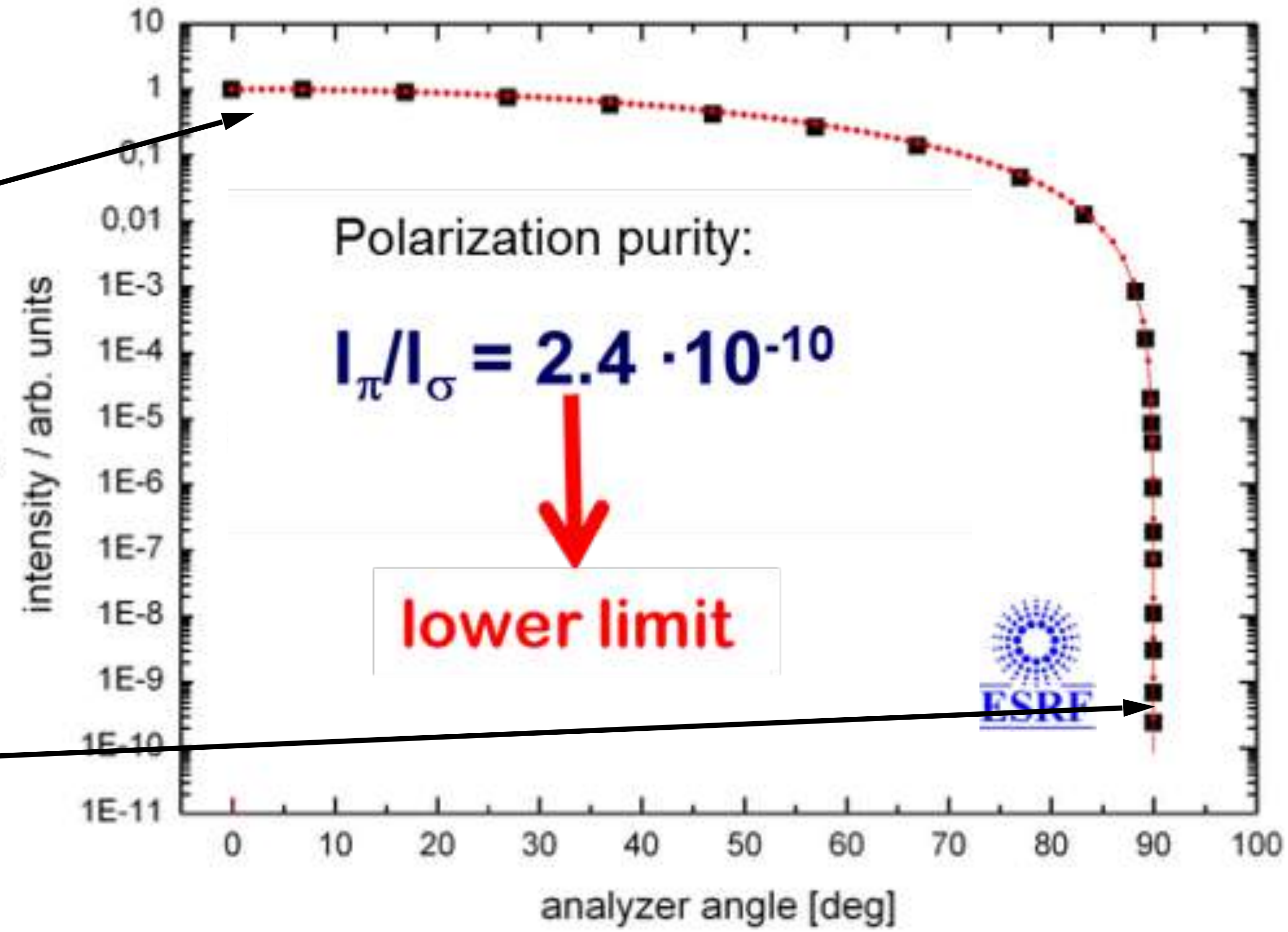

Fig. 9: Polarization purity measurement at E_{ph}= 6.5 keV (λ =1.9 Å) with six reflection Si{004}-channel cut crystals

Marx et al., Phys. Rev. Lett. **110**, 254801 (2013)

limitations: multiple diffraction

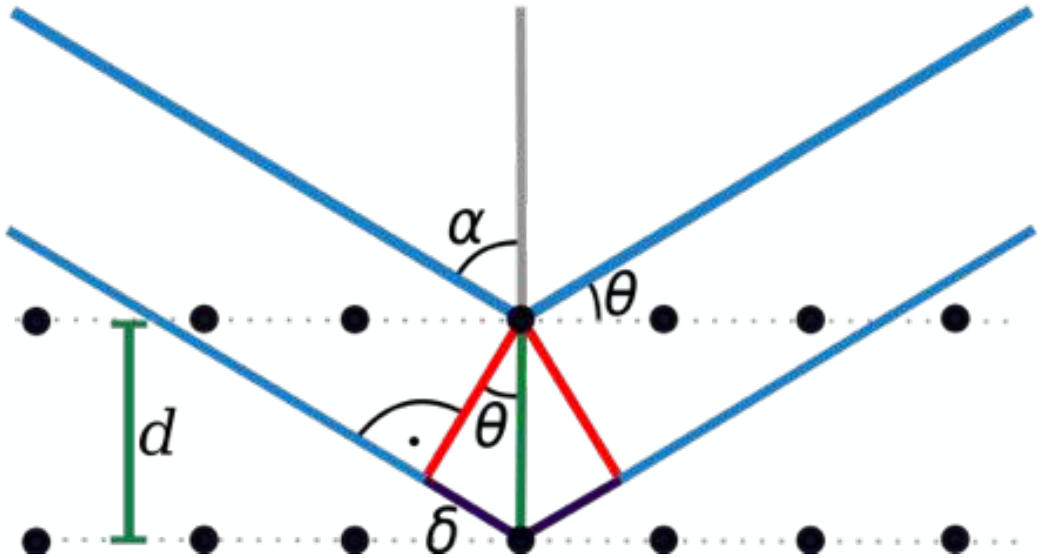

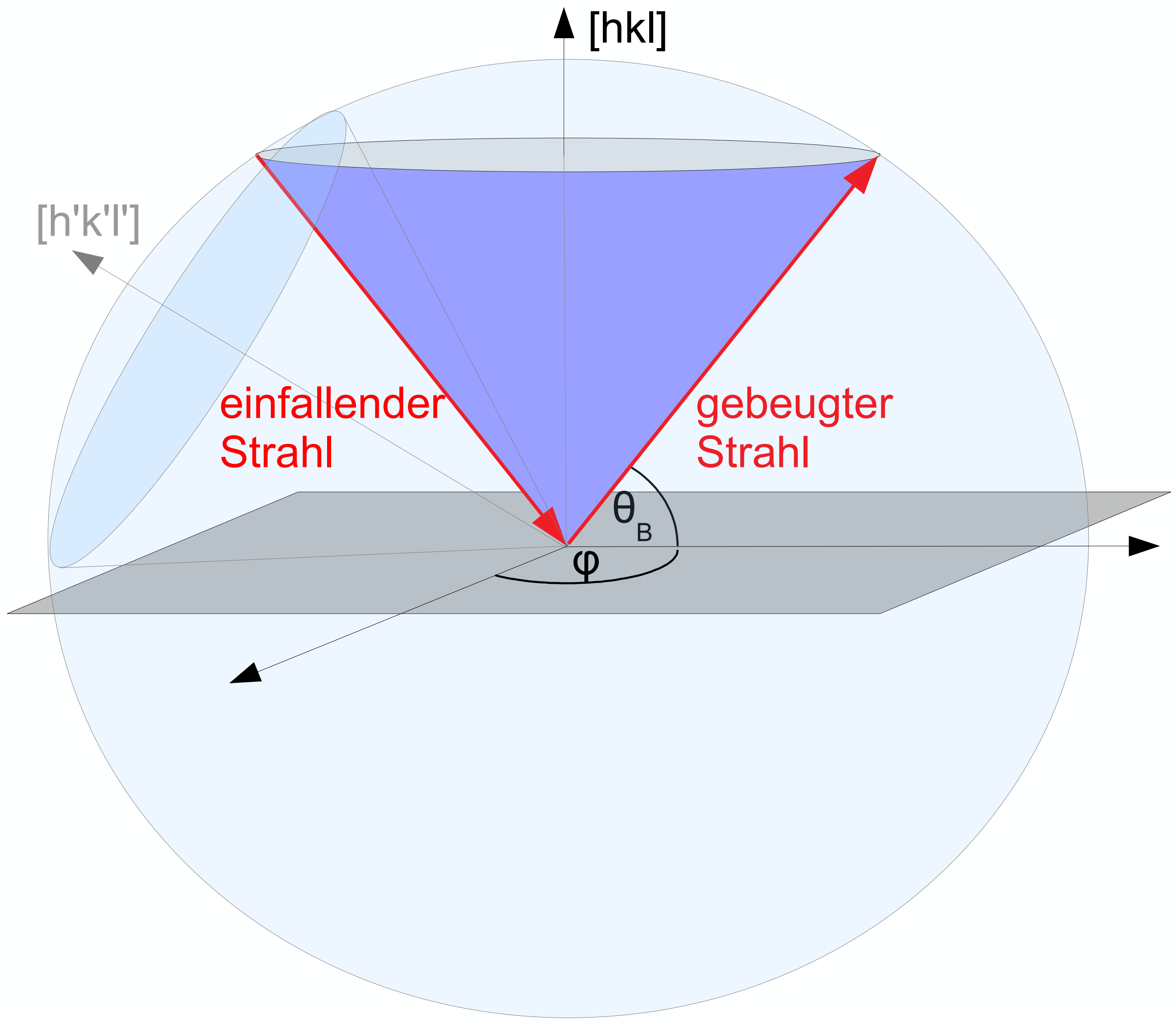

limitations: multiple diffraction

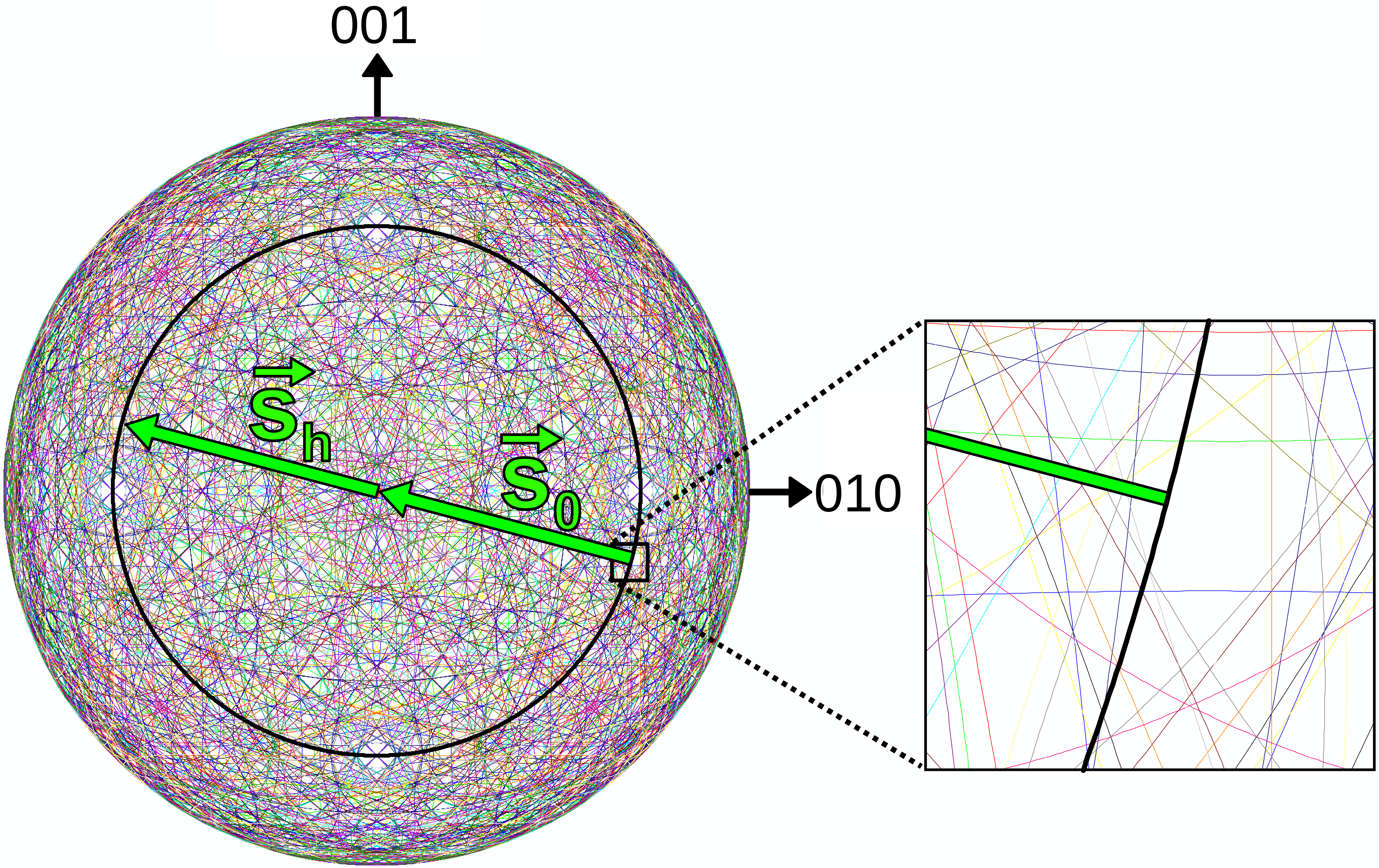

why to use diamond

- smaller lattice parameter
  - Distance between Umweganregungen increases
  - higher photon energy
- less absorption → high reflectivity

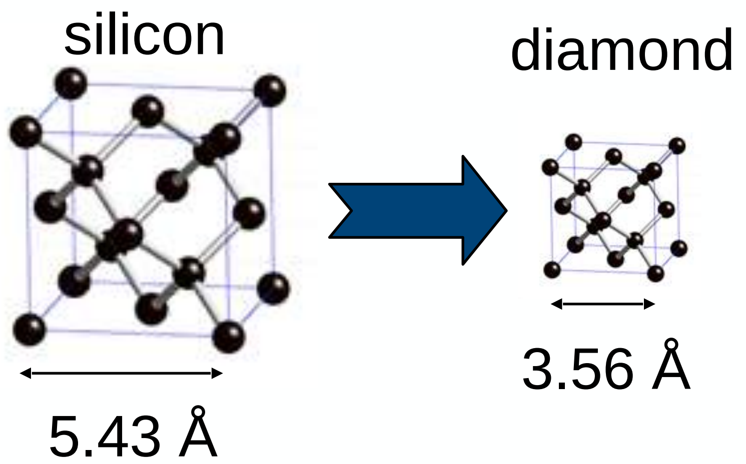

Fig. 14: lattice parameter for silicon & diamond

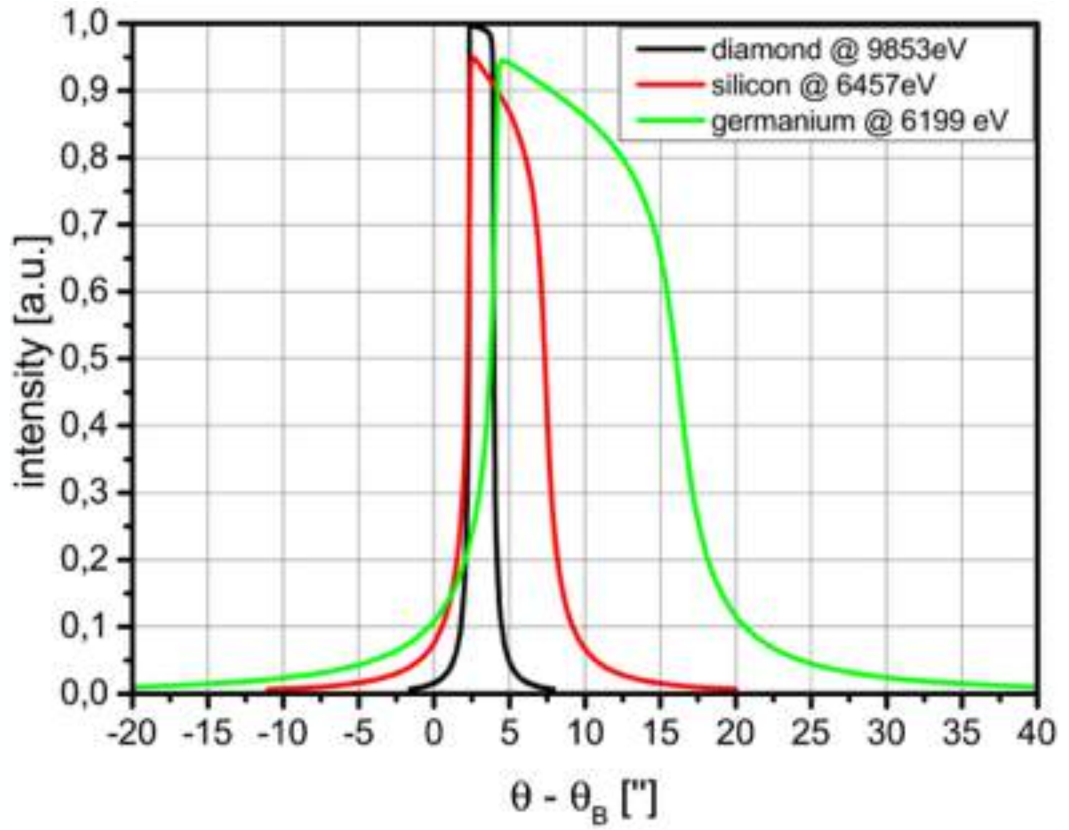

Fig. 15: Calculation of Diamond, Si- & Ge-(004) Darwin-Prince curve @ θ_B=45°

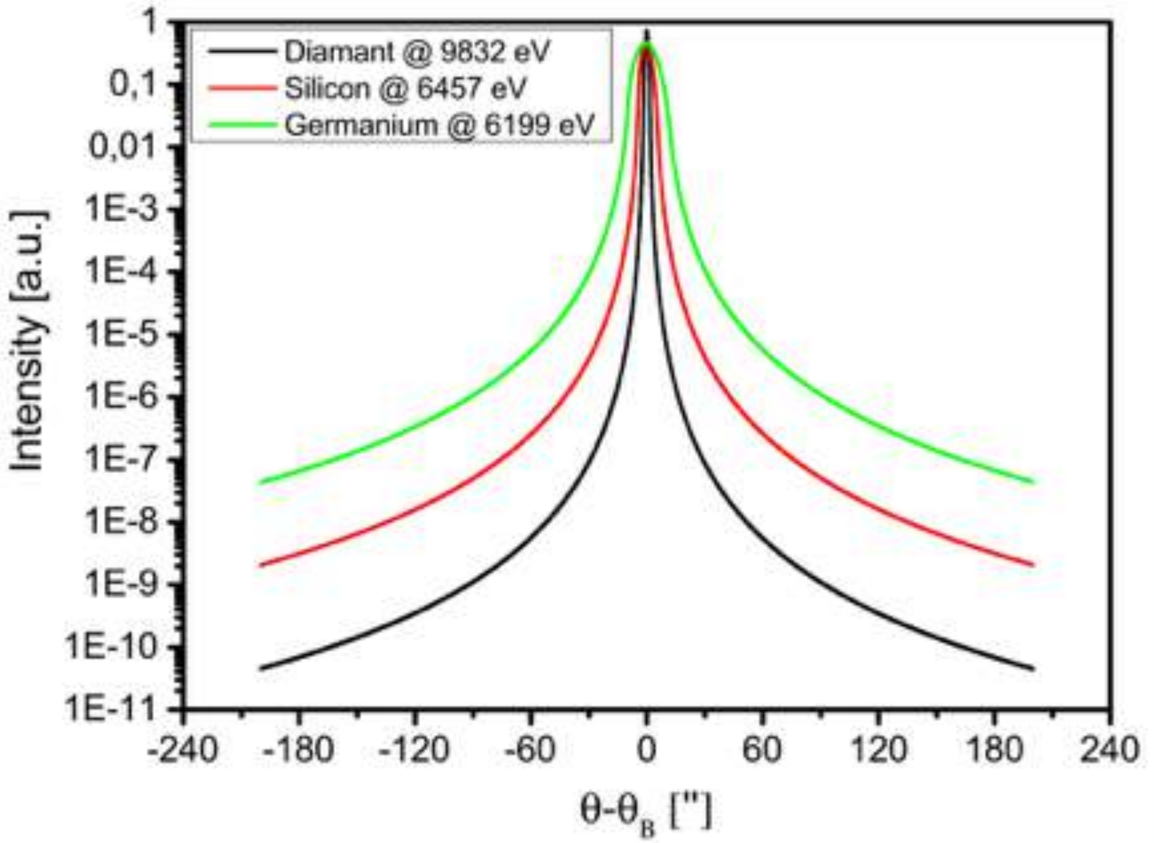

Fig. 16: Calculation of Diamond, Si- & Ge-(004) double crystal rocking curve

why not to use diamond

- expensive → synthetic diamonds
- synthetic diamonds are small
  - no channel-cuts
  - quasi channel cut
- Crystal defects
- available with only one surface orientation

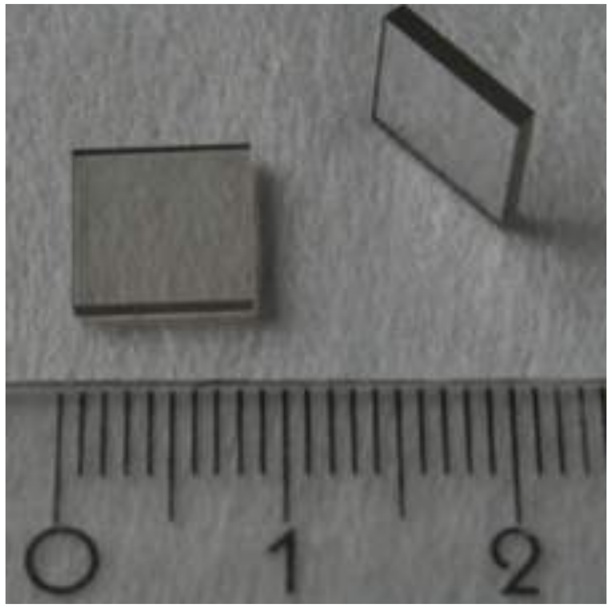

Fig. 17: Synthetic diamonds

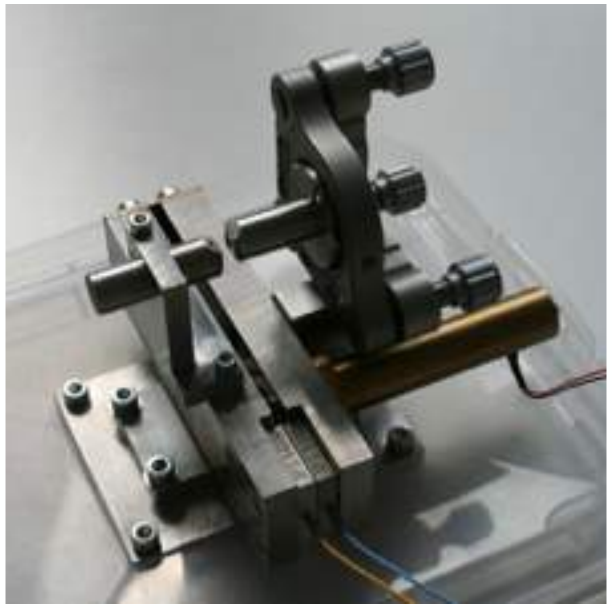

Fig. 18: Quasi channel-cut

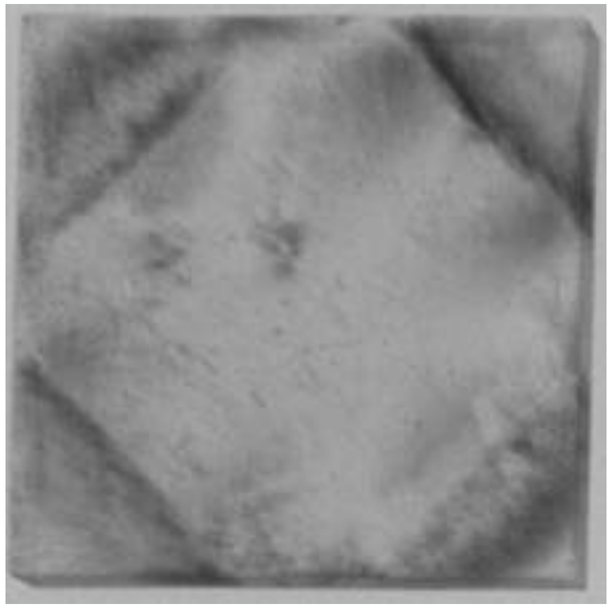

Fig. 19: X-ray topography in transmission geometrie

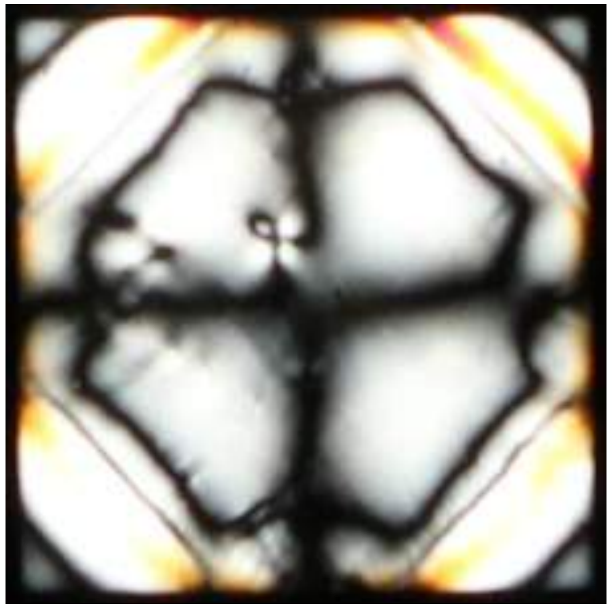

Fig. 20: Stress-induced birefringence observed with polarization microscope

experimental setup

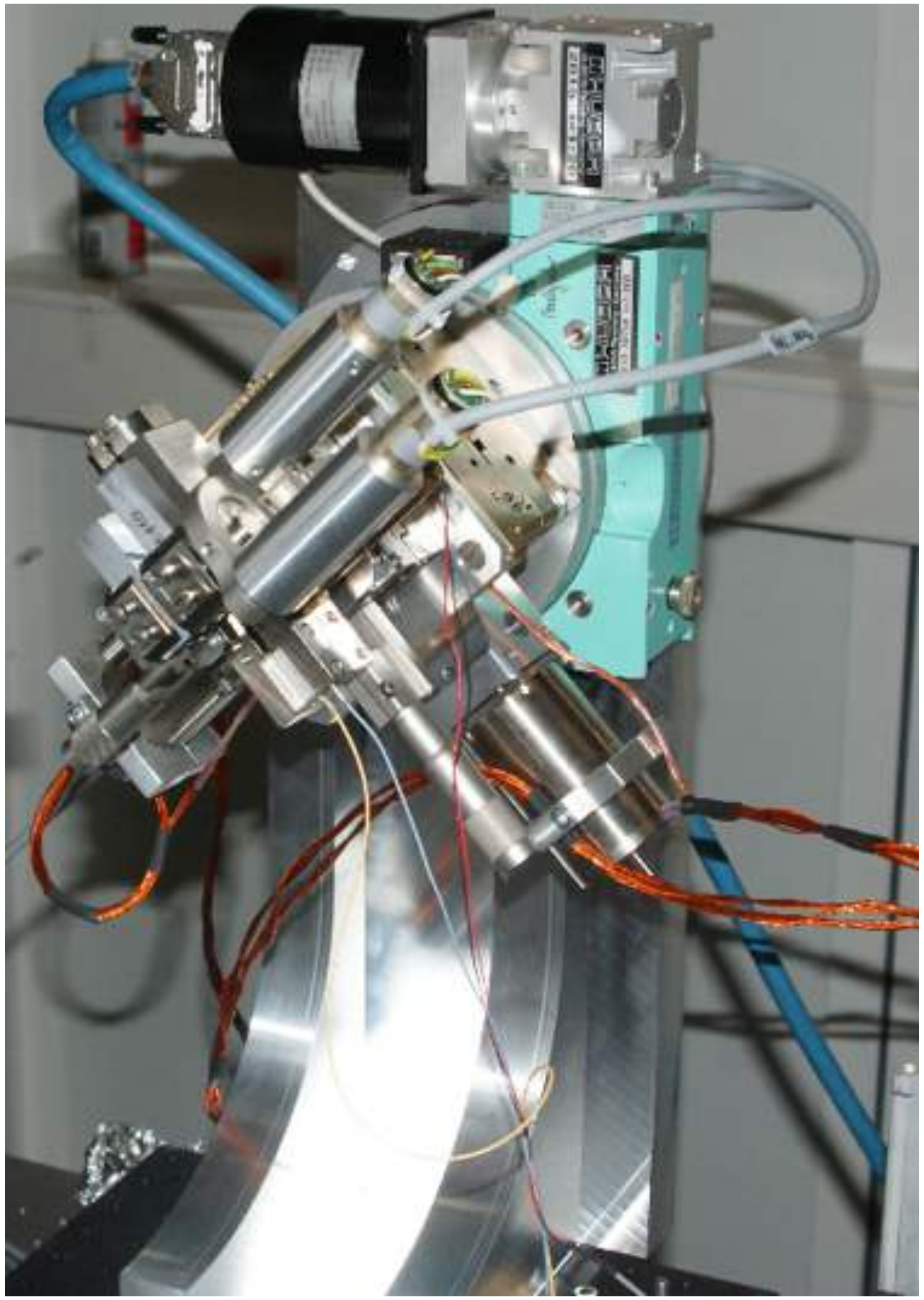

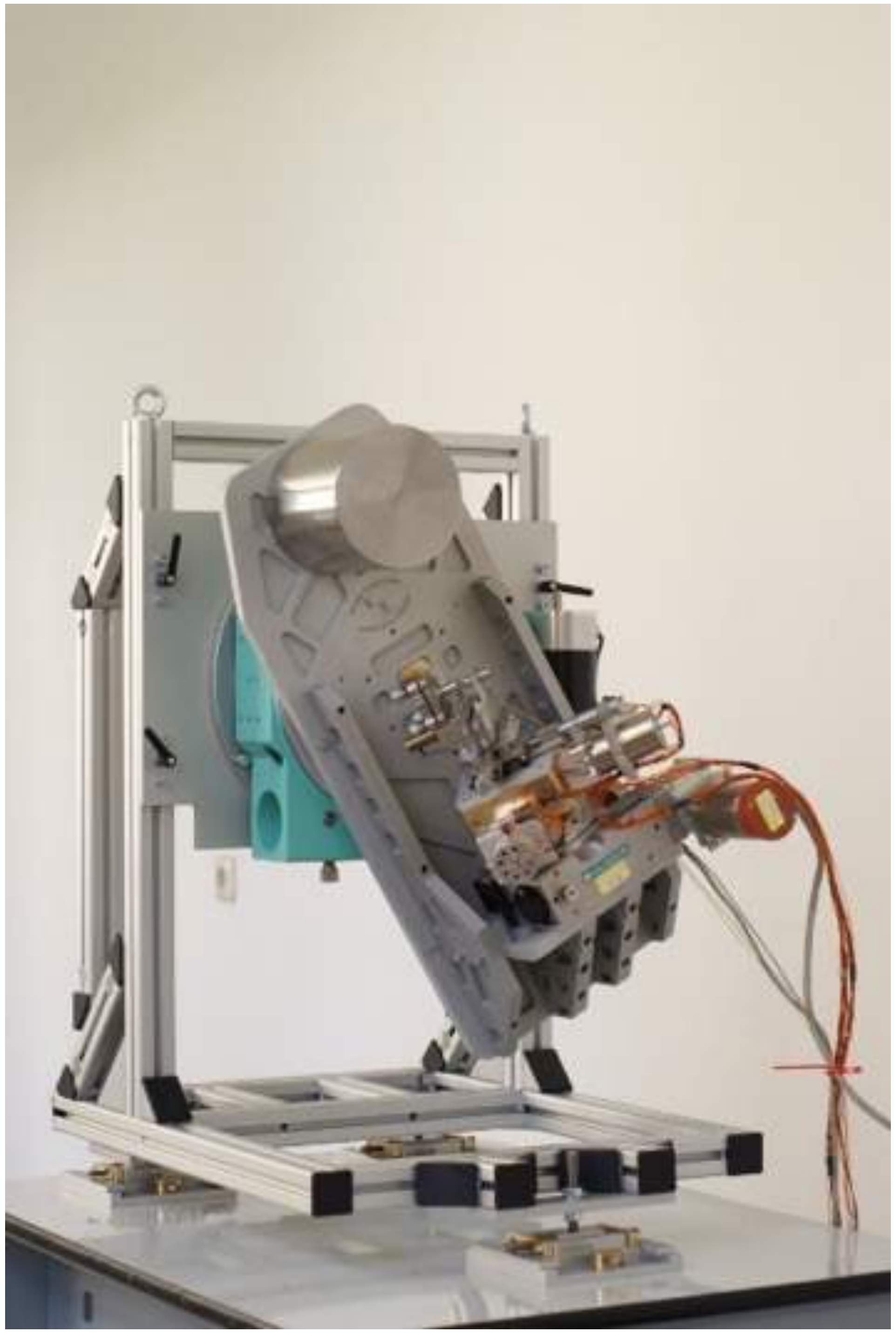

performance of diamond quasi channel-cuts

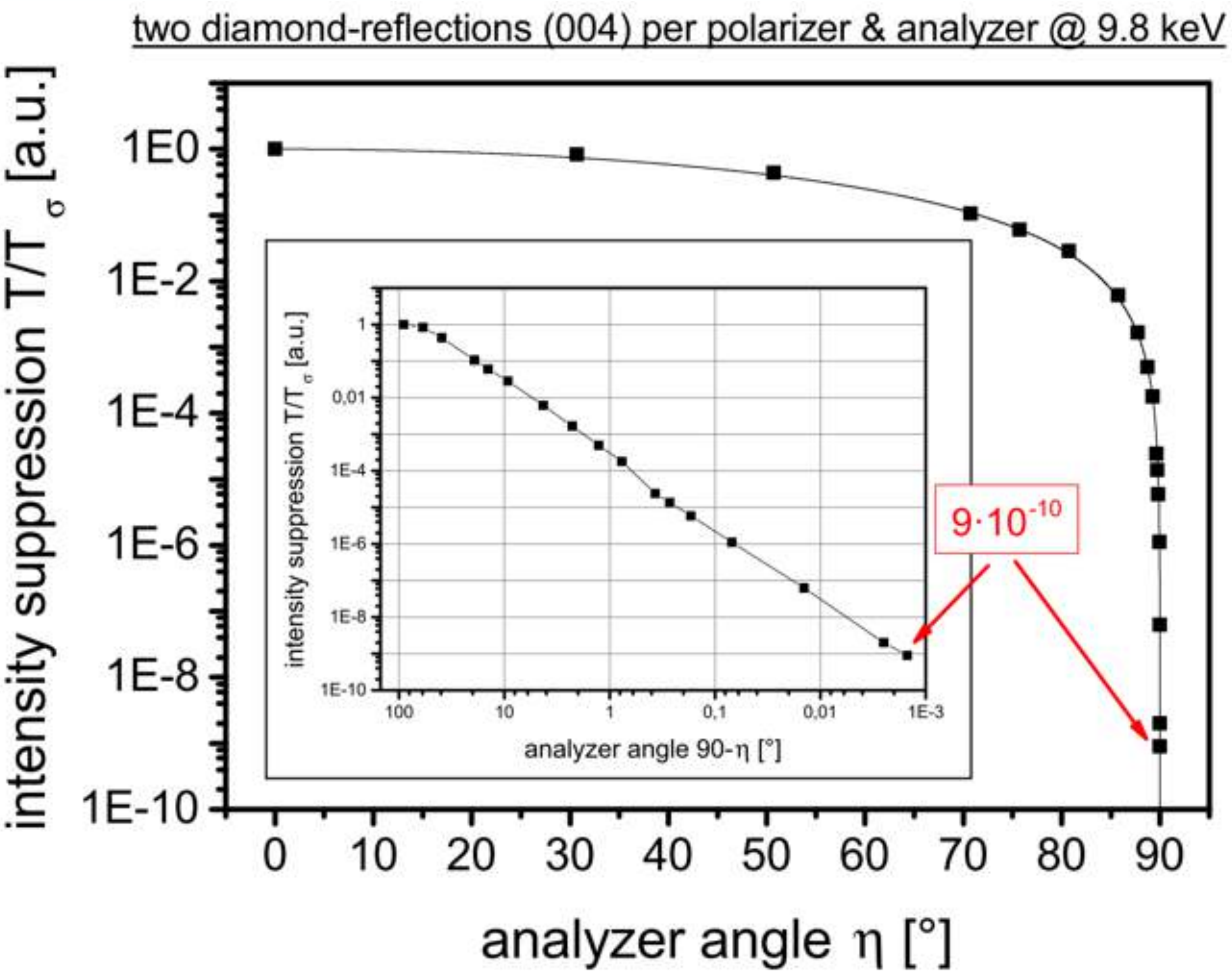

- ionization of ions
  - ion beam apparatus
  - experiments with Ne^+
  - future directions
- high-definition X-ray polarimetry
  - Si channel-cuts
  - diamond quasi channel-cuts